CHALMERS
UNIVERSITY OF TECHNOLOGY

Investigation of efficient and reliable numerical algorithms for coupled reactor calculations

X-TREAM project:

Tasks 3a and 3b – Elaboration of 1-D test cases and comparisons of non-linear inconsistent/consistent methods

Task 4a – Recommendations for non-linear consistent reactor safety simulations

Christophe Demazière[a], Sebastian González-Pintor[b], Anders Ålund[c] and Manuel Calleja[a]

[a] Chalmers University of Technology, Department of Physics, Division of Subatomic and Plasma Physics, SE-412 96 Gothenburg, Sweden

[b] Chalmers University of Technology, Department of Mathematical Sciences, SE-412 96 Gothenburg, Sweden

[c] Fraunhofer Chalmers Research Centre for Industrial Mathematics, Chalmers Science Park, SE-412 88 Gothenburg, Sweden

CTH-NT-332 October 2017

Summary

In this report, some of the work performed in the framework of the X-TREAM project (with X-TREAM standing for neXt generation numerical Techniques for deterministic REActor Modelling) is reported. The work was supported by the Nordic Thermal Hydraulic Network (NORTHNET). The focus of the report is on the tasks 3a and 3b (elaboration of 1-D test cases and comparisons of non-linear inconsistent/consistent methods) and on the task 4a (recommendations for non-linear consistent reactor safety simulations).

A simplified one-dimensional Boiling Water Reactor (BWR) model in steady-state conditions was developed to study the efficiency of the Jacobian-Free Newton Krylov (JFNK) method to solve strongly non-linear multi-physic problems, such as the one corresponding to BWR behaviour, where the interdependence between neutron transport, fluid dynamics and heat transfer needs to be resolved. The modelling assumptions were chosen so that the physics of BWRs could be properly accounted for with an as simple as possible model.

It was found that there is little advantage of solving each of the mono-physics problems using a JFNK approach and iterating between the various solvers until convergence is reached. As noticed with classical operator splitting approaches, such a solver is prone to oscillatory behaviour due to the strong physical coupling between coolant density/fuel temperature and the distributions of neutrons in space/energy. Such oscillations can only be overcome by using some relaxation factor, which results in slow convergence of the overall multi-physics problem.

On the other hand, it was also demonstrated that solving the entire multi-physics problem simultaneously using JFNK is a very powerful technique. The robustness of this technique nevertheless relies on two important aspects: the necessity to create a good enough initial guess to be used by the JFNK algorithm and the need to properly precondition the problem. For the former, using a non-linear Gauss-Seidel technique was proven to provide such an acceptable guess. For the latter, an efficient preconditioner was found to have the following characteristics: separate preconditioning of the neutron transport problem, no preconditioning of the heat transfer problem, preconditioning of the fluid dynamics problem where the cross-dependencies between the void fraction and the phasic velocities are resolved and where the pressure field is treated independently. Based on these characteristics, an analytical preconditioner using first-order (i.e. linear) approximations of the balance equations and relying on a simpler formulation of the problem solved was derived and demonstrated to be efficient. The development of such an analytical preconditioner, which is the key condition to be fulfilled for a multi-physics problem to be solved using a JFNK technique, is nevertheless a major undertaking. The possibility to use a linearly-approximated preconditioner, knowing the structure of the desired preconditioner, was also proposed. It was found to be an interesting alternative when the development of an analytical Jacobian is either too difficult (due to complex models being used in the problem being solved) or when the models are not accessible (“black-box” approach).

Keywords: nuclear reactor modelling, coupled calculations, numerical algorithms, Jacobian-Free Newton Krylov method

Contents

1. Introduction

By essence, nuclear reactors represent multi-physic systems, in which different fields of physics are inter-related. In best-estimate approaches, such interdependent fields are usually restricted to the physics of neutron transport, the physics of fluid dynamics and heat transfer. The simultaneous modelling of these three fields is important both in steady-state conditions as well as in transient conditions. The addition of other fields (fuel behaviour, chemistry, material physics, etc.) might also be necessary in some specific situations.

Typically, the modelling of each physics is done in a segregated manner. One code is used per field at a time, assuming that the other fields are "frozen", and iterations are performed to resolve the interdependences until convergence on all physical fields is achieved [1]. Such a solution strategy is the result of the use of legacy codes developed for modelling each physical field separately, codes that were *à posteriori* coupled to model multi-physics problems. The main advantage of such an *à posteriori* coupling lies with the absence of internal code modification when the code is externally coupled to another software. This results in the preservation of the Verification and Validation (V&V) work for each code. Nevertheless, achieving tight convergence on all physical fields might be difficult and numerical oscillations are often encountered [2]. In addition, when considering transient calculations, the non-linearities are often never fully resolved, resulting in inconsistent coupling algorithms [3].

Other coupling methodologies have recently been proposed, in which the non-linearities can be fully resolved (see [4] for a survey on this subject). One of the most promising approach is the so-called Jacobian-Free Newton Krylov (JFNK) method [4]. This technique gained a lot of attention in recent years for modelling multi-physic problems in nuclear engineering, as can be noticed from the number of scientific publications on this subject.

The present report aims at investigating the performance of a JFNK modelling strategy for Boiling Water Reactor (BWR) conditions, in which the presence of vapor significantly enhances the non-linear effects. Although there have been some successful implementations of JFNK methods in thermal-hydraulic codes for two-phase flow systems [5]-[7], the modelling of coupled neutronics/thermal-hydraulics for BWRs remains largely unexplored. Consequently, a one-dimensional coupled BWR problem was developed in steady-state conditions and was used as a workbench to investigate the performance of the JFNK technique. Emphasis was put on developing an as simple as possible model while retaining the complexity of the system being studied. A simple enough model allows gaining physical insights into the driving mechanisms, which could remain non-trackable when using state-of-the-art modelling tools for coupled BWR physics.

This report is structured as follows. After a brief reminder about the JFNK method, the BWR workbench that was developed is described, together with the main approximations used. Thereafter, comparisons between various multi-physics alternatives and solution strategies are presented. The effect of preconditioning, essential in a JFNK approach, is then touched upon, as well as the generation of a good enough guess to be used in a JFNK technique. Some conclusions and recommendations about the use and applicability of the JFNK method for coupled BWR neutronics/thermal-hydraulics are finally drawn.

2. Reminder about the Jacobian-Free Newton-Krylov Method

The JFNK method was already presented in great details in earlier reports published within this project (see e.g. [4]). Only the essence of the method is recalled hereafter.

The type of problems that need to be numerically solved in nuclear engineering can always be generically formulated as:

$$\mathbf{F}\left(\mathbf{x}\right) = 0 \tag{1}$$

where $\mathbf{x}$ is a vector containing n unknown variables and $\mathbf{F}$ represents n balance equations relating the n unknown variables. These n balance equations usually contain non-linear dependences between the unknown variables.

Making a first-order Taylor expansion of $\mathbf{F}$ near $\mathbf{x}_0$ leads to:

$$\mathbf{F}\left(\mathbf{x}\right) \approx \mathbf{F}\left(\mathbf{x}_0\right) + \mathbf{J}\left(\mathbf{x}_0\right)\left[\mathbf{x} - \mathbf{x}_0\right] \tag{2}$$

where $\mathbf{J}\left(\mathbf{x}_0\right)$ represents the Jacobian of the function $\mathbf{F}$ in $\mathbf{x}_0$. Using Eq. (1) and rearranging gives:

$$\mathbf{J}\left(\mathbf{x}_0\right)\left[\mathbf{x} - \mathbf{x}_0\right] \approx -\mathbf{F}\left(\mathbf{x}_0\right) \tag{3}$$

and

$$\mathbf{x} \approx \mathbf{x}_0 - \left[\mathbf{J}\left(\mathbf{x}_0\right)\right]^{-1} \mathbf{F}\left(\mathbf{x}_0\right) \tag{4}$$

Assuming that $\mathbf{x}_0$ is a given start vector, Eq. (4) defines an iterative process that can be more explicitly written as:

$$\mathbf{x}^{k+1} \approx \mathbf{x}^{k} - \left[\mathbf{J}\left(\mathbf{x}^{k}\right)\right]^{-1} \mathbf{F}\left(\mathbf{x}^{k}\right) \tag{5}$$

where k is the iteration number. This iterative scheme, referred to as a Newton or Newton-Raphson method [8], leads to a new state vector $\mathbf{x}^{k+1}$ that, under given conditions, should be closer to the actual root of Eq. (1) than $\mathbf{x}^{k}$ is. Although this method is often used for solving non-linear problems, it requires at each new iteration both the actual evaluation of the Jacobian and its inversion. Depending of the number of state variables, these tasks can be computationally very expensive.

The essence of the JFNK method is to reformulate the above problem as:

$$\mathbf{J}\left(\mathbf{x}^{k}\right)\delta\mathbf{x}^{k} = -\mathbf{F}\left(\mathbf{x}^{k}\right) \tag{6}$$

with

$$\delta\mathbf{x}^{k} = \mathbf{x}^{k+1} - \mathbf{x}^{k} \tag{7}$$

and not performing the actual evaluation of the Jacobian and its inversion. This is achieved by noticing that Eq. (6) is equivalent to a linear algebra problem of the form $\mathbf{A} \times \mathbf{v} = \mathbf{b}$ where $\mathbf{A}$ and $\mathbf{b}$ represent a given matrix and a given vector, respectively, and $\mathbf{v}$ is thus the state vector solution to the equation $\mathbf{A} \times \mathbf{v} = \mathbf{b}$. This type of equation can be very efficiently solved using a Krylov subspace method [9].

Within each Newton iteration k, a second iterative scheme is thus applied. It consists of the construction of a Krylov subspace of dimension m:

$$\mathbf{K}_m = span\left\{\mathbf{r}_0, \mathbf{J}\left(\mathbf{x}^k\right)\mathbf{r}_0, \left[\mathbf{J}\left(\mathbf{x}^k\right)\right]^2 \mathbf{r}_0, ..., \left[\mathbf{J}\left(\mathbf{x}^k\right)\right]^{m-1} \mathbf{r}_0\right\} \tag{8}$$

with

$$\mathbf{r}_0 = -\mathbf{F}\left(\mathbf{x}^k\right) - \mathbf{J}\left(\mathbf{x}^k\right)\delta\mathbf{x}_0 \tag{9}$$

and on the use of an orthogonalizing technique, such as the Generalized Minimal Residual method (GMRES) to update the vector $\delta\mathbf{x}_0$ so that it approaches the true solution $\delta\mathbf{x}^k$ of Eq. (6) [10].

The main advantage of combining a Krylov subspace method with the Newton method lies with the fact that no formal evaluation of the Jacobian matrix is required. Instead, only the products between the Jacobian and vectors (thus resulting in vectors) are necessary for the construction of the Krylov subspace, as can be noticed in Eq. (8). This leads to a much lower computational effort compared to the evaluation of the full Jacobian. In addition, the product between the Jacobian and a vector can be further approximated as e.g.:

$$\mathbf{J}\left(\mathbf{x}^k\right)\mathbf{v} \approx \left[\mathbf{F}\left(\mathbf{x}^k + \varepsilon\mathbf{v}\right) - \mathbf{F}\left(\mathbf{x}^k\right)\right] / \varepsilon \tag{10}$$

using a first-order Taylor expansion and where ε is a small perturbation.

3. Presentation of the developed workbench

In this Section, the models that were retained for developing a coupled numerical framework aimed at studying the performances and applicability of the JFNK method for BWR applications are presented. The incentives in the choice of the different modelling assumptions were to develop an as simple as possible set of models being still representative of the physics of BWRs. One of the peculiarities of the modelling of BWRs is the strong dependence of both the macroscopic cross-sections and the thermal-hydraulic correlations on the void fraction and/or the flow regimes. Special attention was thus put on preserving this feature in the modelling assumptions used.

Emphasis of the workbench was put on the coupling existing between the neutronics and the thermal-hydraulics in steady-state conditions. The retained neutron transport model was thus based on a two-group diffusion theory formalism (as used in standard core simulators). The fluid dynamics model was built upon a mixture formulation assuming thermal equilibrium between the liquid and vapor phases and using a specified drift velocity between the phases (model referred to as a "four-equation" model in the literature). The modelling of heat conduction in the fuel pins was carried out by radially-averaging the temperature on the fuel and cladding regions, respectively. In order to simplify the model as much as possible, only the axial direction was retained (one-dimensional modelling).

a. Cross-section modelling

The macroscopic cross-sections and diffusion coefficients necessary to the neutron transport calculations were generated in advance and processed so that they could be directly used in the developed workbench. These data were created from CASMO-4E calculations [11] performed in an earlier project [12].

A two-dimensional model of a SVEA 96 BWR fuel assembly containing six fuel pins with Gadolinium oxide was considered in an infinite lattice set-up, with a critical spectrum correction to account for the effect of neutron leakage. The calculations were performed with a 70-group nuclear data library essentially based on ENDF/B-VI. Not control rod was assumed to be inserted in the fuel assembly. The calculations were performed at fresh conditions, in order to avoid the unnecessary complication of the modelling of the dependencies on history effects.

The following data were then created as functions of coolant density and fuel temperature, on a range of [0.037 – 0.835] g/cm^3 and [538 – 938] K, respectively:

- The thermal diffusion coefficient D_1.
- The fast diffusion coefficients D_2.

- The macroscopic removal cross-section Σ_{rem} (defined as the isotropic downscattering cross-section minus the isotropic upscattering cross-section weighted with the ratio between the thermal and the fast neutron fluxes).
- The fast macroscopic absorption cross-section $\Sigma_{a,1}$.
- The thermal macroscopic absorption cross-section $\Sigma_{a,2}$.
- The average number of neutrons released per fission event υ .
- υ times the fast macroscopic fission cross-section $\Sigma_{f,1}$.
- υ times the thermal macroscopic fission cross-section $\Sigma_{f,2}$.
- The average energy released by per fission event κ .

Two-dimensional spline interpolation functions between the created data points were then built with respect to the coolant density and the fuel temperature. Spline extrapolations were performed when calling a coolant density value and/or a fuel temperature value outside of the ranges of the created data point values. An example of the functionalization of the macroscopic data on coolant density and fuel temperature is given in Fig. 1 for the macroscopic thermal absorption cross-section.

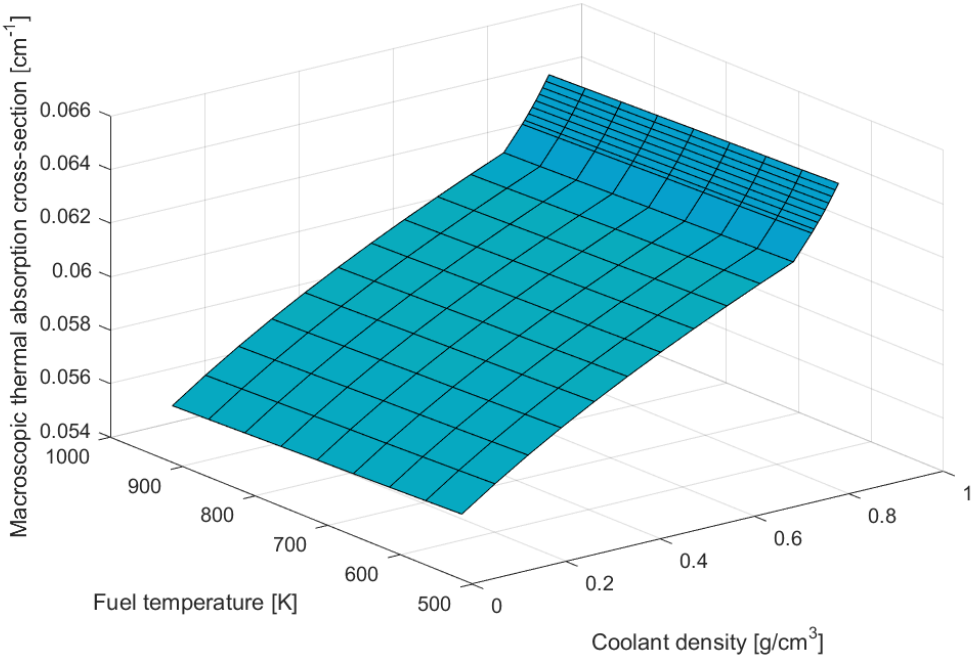

Fig. 1 Dependence of the macroscopic thermal absorption cross-section as a function of fuel temperature and coolant density (reconstructed from CASMO-4E simulations).

b. Neutron transport modelling

The modelling of neutron transport was performed using a low-order method based on diffusion theory. This method only resolves the first moments of the angular neutron flux, namely the scalar neutron flux and the neutron current density vector. In addition, the energy discretization was based on a two-energy group formulation.

Using standard notations, the balance equations for the fast energy group and the thermal energy group, respectively, read as:

$$\begin{cases} -\bar{\nabla}\cdot\mathbf{J}_1(\mathbf{r}) + \frac{1}{k}\sum_{g'=1}^{2}\left(\upsilon\Sigma_f\right)_{g'}(\mathbf{r})\phi_{g'}(\mathbf{r}) - \Sigma_{a,1}(\mathbf{r})\phi_1(\mathbf{r}) - \Sigma_{rem}(\mathbf{r})\phi_1(\mathbf{r}) = 0 \\ -\bar{\nabla}\cdot\mathbf{J}_2(\mathbf{r}) - \Sigma_{a,2}(\mathbf{r})\phi_2(\mathbf{r}) + \Sigma_{rem}(\mathbf{r})\phi_1(\mathbf{r}) = 0 \end{cases} \tag{11}$$

with

$$\begin{cases} \mathbf{J}_1(\mathbf{r}) = -D_1(\mathbf{r})\bar{\nabla}\phi_1(\mathbf{r}) \\ \mathbf{J}_2(\mathbf{r}) = -D_2(\mathbf{r})\bar{\nabla}\phi_2(\mathbf{r}) \end{cases} \tag{12}$$

and where it was assumed that all neutrons released by fission are emitted in the fast energy group. Eqs. (11) and (12) can be more compactly written:

$$\begin{cases} \bar{\nabla}\cdot\left[D_1(\mathbf{r})\bar{\nabla}\phi_1(\mathbf{r})\right] + \frac{1}{k}\sum_{g'=1}^{2}\left(\upsilon\Sigma_f\right)_{g'}(\mathbf{r})\phi_{g'}(\mathbf{r}) - \Sigma_{a,1}(\mathbf{r})\phi_1(\mathbf{r}) - \Sigma_{rem}(\mathbf{r})\phi_1(\mathbf{r}) = 0 \\ \bar{\nabla}\cdot\left[D_2(\mathbf{r})\bar{\nabla}\phi_2(\mathbf{r})\right] - \Sigma_{a,2}(\mathbf{r})\phi_2(\mathbf{r}) + \Sigma_{rem}(\mathbf{r})\phi_1(\mathbf{r}) = 0 \end{cases} \tag{13}$$

k is the eigenvalue corresponding to the eigenvector $\left[\phi_1(\mathbf{r});\phi_2(\mathbf{r})\right]$. An infinite number of solutions exist. The solution having the largest k value corresponds to the fundamental mode of the system and the k value thus corresponds to the effective multiplication factor of the system, i.e. k_{eff}. It can be noticed that since both the eigenvalue and the eigenvector are unknown quantities, the system of equations can be considered as a non-linear system of equations.

Concerning the spatial discretization of the system of equations above, finite differences were used, resulting in the following system of equations:

$$\begin{cases} \left(a_{1,n}\phi_{1,n} + b_{1,n}\phi_{1,n+1} + c_{1,n}\phi_{g,n-1}\right) + \Sigma_{a,1,n}\phi_{1,n} + \Sigma_{rem,n}\phi_{1,n} = \frac{1}{k}\left[\left(\upsilon\Sigma_f\right)_{1,n}\phi_{1,n} + \left(\upsilon\Sigma_f\right)_{2,n}\phi_{2,n}\right] \\ \left(a_{2,n}\phi_{2,n} + b_{2,n}\phi_{2,n+1} + c_{2,n}\phi_{2,n-1}\right) + \Sigma_{a,2,n}\phi_{2,n} = \Sigma_{rem,n}\phi_{1,n} \end{cases} \tag{14}$$

where the coupling coefficients are given as[1]:

[1] It has to be noted that the expressions of the coupling coefficients given in Eq. (15) assume that the node n has two neighbours (i.e. node $n-1$ and node $n+1$). For a node n located at either the lower or upper boundary of the system, the expressions are slightly different. For the sake of clarity, these expressions are not recalled here. We refer instead to e.g. [13].

$$\begin{cases} a_{g,n} = \dfrac{2D_{g,n-1}D_{g,n}}{\left(\Delta z\right)^2\left(D_{g,n-1}+D_{g,n}\right)} + \dfrac{2D_{g,n}D_{g,n+1}}{\left(\Delta z\right)^2\left(D_{g,n}+D_{g,n+1}\right)} \\ b_{g,n} = -\dfrac{2D_{g,n}D_{g,n+1}}{\left(\Delta z\right)^2\left(D_{g,n}+D_{g,n+1}\right)} \\ c_{g,n} = -\dfrac{2D_{g,n-1}D_{g,n}}{\left(\Delta z\right)^2\left(D_{g,n-1}+D_{g,n}\right)} \end{cases} \text{, for } g = 1,2 \qquad (15)$$

with Δz representing the mesh size in the retained axial direction (one-dimensional modelling). Solving the above system of equations thus allows determining the axial variation of the fast neutron flux $\phi_{1,n}$ and thermal neutron flux $\phi_{2,n}$ for every axial node $n = \left[1,2,...,N-1,N\right]$ (with N being the total number of nodes in the axial direction), together with k_{eff}, the effective multiplication factor of the system. The vector of unknown quantities can thus be expressed as $\left[\phi_{1,1};...;\phi_{1,N};\phi_{2,1};...;\phi_{2,N};k_{eff}\right]^T$.

c. Fluid dynamics modelling

The modelling of the fluid properties was carried out using a mixture model formulation of the local conservation equations for mass, linear momentum, and enthalpy, assuming thermal equilibrium between the liquid and vapour phases and identical pressure for both phases. Some drift between the velocities of the vapour phase and of the liquid phase was allowed, using an algebraic relationship proposed by Zuber and Findlay [14] with some simplifications. Using standard notations and after volume- and time-averaging, the conservation equations, often referred to as a four-equation model in the literature, read in steady-state conditions as (see [15] for further details):

$$\begin{gathered} \overline{\nabla}\cdot\left(\beta\overline{G}_m\right) = 0 \\ \overline{\nabla}\cdot\left(\beta\overline{G}_m \otimes \overline{v}_m\right) + \overline{\nabla}\cdot\left(\beta\left\langle\underline{\alpha}\right\rangle\left(1-\left\langle\underline{\alpha}\right\rangle\right)\frac{\hat{\rho}_l\hat{\rho}_v}{\rho_m}\left(\overline{v}_r \otimes \overline{v}_r\right)\right) \approx \beta\rho_m\overline{g} - \beta\overline{\nabla}\hat{P} + \sum_{k=l,v}\overline{F}_{kw} \\ \overline{\nabla}\cdot\left(\beta\overline{G}_m h_m\right) + \overline{\nabla}\cdot\left(\beta\left\langle\underline{\alpha}\right\rangle\left(1-\left\langle\underline{\alpha}\right\rangle\right)\frac{\hat{\rho}_l\hat{\rho}_v}{\rho_m}\left(\overline{v}_r h_r\right)\right) \approx \beta\left\{\overline{J}_m\cdot\overline{\nabla}\hat{P}\right\} + \sum_{k=l,v}E_{kw} \\ \hat{\overline{v}}_v = \overline{\overline{C}}_0\overline{J}_m + \overline{V}_{vj} \end{gathered} \qquad (16)$$

where the drift velocity is given as the difference between the velocity of the vapour phase and the velocity of the liquid phase:

$$\overline{v}_r = \hat{\overline{v}}_v - \hat{\overline{v}}_l \qquad (17)$$

The above set of equations was obtained by further neglecting (see [15] for further details):

- In the momentum conservation equation: the effect of internal stresses and of their turbulent component.
- In the enthalpy conservation equation: the volumetric heat sources, the work of the forces due to phase change and pressure/stresses at the interface and at the solid walls; the kinetic energy due to mass variation in case of phase change; the viscous and turbulent dissipation terms; the effect of internal heat flux and of their turbulent component.

In the present work, it was further assumed that the coolant entered the heated channel at saturated conditions directly. The existence of the one-phase region at the bottom of BWR fuel assemblies was thus neglected, since this region is small compared to the entire length of the channel.

A simplified water table derived from the MATLAB function `IAPWS-IF97.m` [16] (itself essentially using the data from [17]) was created. Concerning the modelling of pressure drops due to friction, a two-phase friction factor based on the method of Lockhart-Martinelli (Eqs. 11-86 to 11-95 in [18]) was used.

For the actual correlations implemented in the drift flux model, a simplified version of the Zuber and Findlay model was developed (using some data from Table 11-2 in [18]). This model can be stated as follows:

- Bubbly flow exists for a void fraction $\langle \underline{\alpha} \rangle$ lying in the interval [0; 0.15] for which the following correlations can be used for the Zuber and Findlay drift flux model:

$$C_0 = 1.2 \text{ and } V_{vj} = \left(1 - \langle \underline{\alpha} \rangle\right)^{1.5} \times V_\infty \tag{18}$$

  with

$$V_\infty = 1.53 \times \left(\sigma g \times \frac{\hat{\rho}_l - \hat{\rho}_v}{\hat{\rho}_l^2} \right)^{1/4} \tag{19}$$

  in which σ represents the surface tension being equal in the present case to 0.01763 kg.s^{-2}.

- Churn flow exists for a void fraction $\langle \underline{\alpha} \rangle$ lying in the interval]0.15; 0,25] for which the following correlations can be used for the Zuber and Findlay drift flux model:

$$C_0 = 1.2 \text{ and } V_{vj} = V_\infty \tag{20}$$

  with V_∞ given by Eq. (19).

- Slug flow exists for a void fraction $\langle \underline{\alpha} \rangle$ lying in the interval]0.25; 1] for which the following correlations can be used for the Zuber and Findlay drift flux model:

$$C_0 = 1.2 \text{ and } V_{vj} = V_\infty \tag{21}$$

  with

$$V_{\infty} = 0.35 \times \left(g \times \frac{\hat{\rho}_l - \hat{\rho}_v}{\hat{\rho}_l} \times D_e \right)^{1/2} \tag{22}$$

in which $D_e = 4A / P_w$ represents the equivalent hydraulic diameter.

The model detailed above does not consider flow regimes beyond slug flows. Although this represents a major simplification compared to the actual flow regimes actually encountered in the upper part of BWR fuel assemblies, this allows to categorize the flow regimes entirely on the knowledge of the void fraction $\left\langle \underline{\alpha} \right\rangle$. For the present work, aimed at developing a simple enough model catching the features of the modelling of BWR physics, the dependence of the flow regimes on the void fraction preserves the existence of discontinuities in the use of correlations between various flow regimes (in the present case, bubbly, slug and churn flows).

The set of equations in (16) was then solved assuming a mono-directional moving fluid in the upper direction along the fuel assembly and the spatial discretization was performed using finite differences. The divergence terms of any vector quantity $\overline{c}$ averaged on a control volume V of length Δz and surface area A in a mono-directional formulation further reduces to:

$$\overline{\nabla} \cdot \left\langle \overline{c} \right\rangle = \overline{\nabla} \cdot \left\langle c\overline{z} \right\rangle = \frac{\partial}{\partial z} \left\langle c \right\rangle = \frac{1}{\Delta z} \left[\left\{ c \right\} \left(z + \frac{\Delta z}{2} \right) - \left\{ c \right\} \left(z - \frac{\Delta z}{2} \right) \right] \tag{23}$$

where the last equality was obtained noticing that the spatial derivative of a volume-average quantity can be replaced by the difference between two area-averaged quantities at the upper and lower boundaries, respectively, of the considered volume. In Eq. (23), the volume-averaged terms are denoted with $\left\langle \ \right\rangle$, whereas the area-averaged terms are denoted with $\left\{ \ \right\}$.

Because the balance equations then contain both volume-averaged quantities and area-averaged quantities, all volume-averaged quantities were approximated by the mean of the upper and lower area-averaged quantities for each node, i.e.

$$\left\langle c \right\rangle = \frac{1}{2} \left[\left\{ c \right\} \left(z + \frac{\Delta z}{2} \right) + \left\{ c \right\} \left(z - \frac{\Delta z}{2} \right) \right] \tag{24}$$

Using the water tables and all the correlations mentioned above, the entire set of equations was formulated using as primary unknown variables the void fraction $\underline{\alpha}$, the velocity of the liquid phase v_l, the velocity of the vapour phase v_v, and the pressure $\hat{P}$ at the node interfaces. The vector of unknown quantities, thus expressed as area-averaged quantities can be expressed as $\left[\left\{ \underline{\alpha} \right\}_{1+1/2}; \ldots; \left\{ \underline{\alpha} \right\}_{N+1/2}; \left\{ v_l \right\}_{1+1/2}; \ldots; \left\{ v_l \right\}_{N+1/2}; \left\{ v_v \right\}_{1+1/2}; \ldots; \left\{ \overline{v}_v \right\}_{N+1/2}; \left\{ \hat{P} \right\}_{1/2}; \ldots; \left\{ \hat{P} \right\}_{N-1/2} \right]^T$. It has to be noted that boundary conditions for the void fraction and phasic velocities are imposed at the bottom of the fuel channel, whereas the pressure is imposed at the top of the fuel channel. As can be seen in the vector formulation of the unknown quantities, the void

fraction and phasic velocities need to be determined from the upper interface of the lowermost node to the top of the fuel channel, whereas the pressure needs to be determined from the bottom of the fuel channel to the lower interface of the uppermost node.

d. Heat transfer modelling

The modelling of the heat transferred from the fuel to the coolant was performed in the simplest possible manner, while preserving the physics at hand and paying attention to the necessary coupling mechanisms existing with the physics of neutron transport and of fluid dynamics. The modelling was thus carried out by analytically solving for the radial temperature profile existing in the fuel pins and in the cladding, while representing the heat transfer through the gap via an equivalent heat transfer coefficient. The radial temperature profiles were thus radially averaged to obtain radially-averaged temperatures for the fuel pellets and for the cladding, respectively. Such an averaging process was performed for each axial node of the system, so that the axial temperature profiles could be reconstructed.

Considering an axial slice of a fuel pin (equivalent to a system being infinite in the axial direction) and its radial sketch as represented in Fig. 2, the heat transfer problem becomes mono-dimensional. The temperature profiles can be expressed as functions of the distance from the centre r of the fuel pin. Starting with the heat conduction equation written, using standard notations, in the fuel pellet and in the cladding, respectively as:

$$k_f \bar{\nabla}^2 T_f\left(r\right) + q''' = 0 \tag{25}$$

and

$$k_c \bar{\nabla}^2 T_c\left(r\right) = 0 \tag{26}$$

the temperature profiles are found to be expressed in the fuel pellet and in the cladding, respectively as:

$$T_f\left(r\right) = T_{f,max} - \frac{q''' r^2}{4k_f} \tag{27}$$

and

$$T\left(r\right) = T_{ci} - \frac{R_{ci} q_{ci}'''}{k_c} \ln\left(\frac{r}{R_{ci}}\right) \tag{28}$$

The equations above were obtained by further neglecting the dependence of the fuel thermal conductivity k_f and of the cladding thermal conductivity k_c on the temperature profile being resolved. It will be seen later that the developed solver nevertheless accounts for the dependence of these two conductivities on the radially-averaged temperature profiles in each of these two regions, respectively.

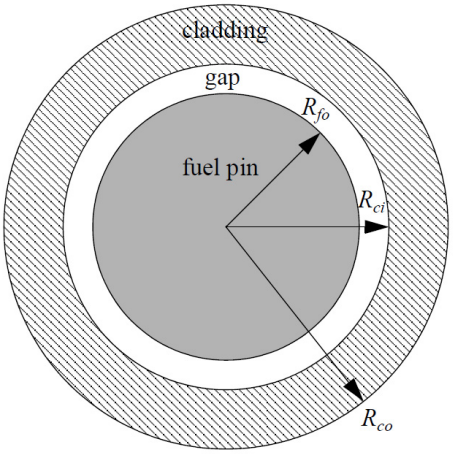

Fig. 2 Sketch of a fuel pin, its surrounding cladding, and the associated gap (for reasons of clarity of the sketch, the cladding and the gap were enlarged).

Using an equivalent heat transfer coefficient h_g for the gap and describing the heat being transferred between the outer periphery of the cladding and the coolant by a heat transfer coefficient h, one finds (see [19] for the details of the derivation):

$$T_{f,max} - T_m = R_{eff} \times q' \tag{29}$$

with

$$R_{eff} = \frac{1}{4\pi k_f} + \frac{1}{2\pi R_g h_g} + \frac{1}{2\pi k_c} \ln\left(\frac{R_{co}}{R_{ci}}\right) + \frac{1}{2\pi R_{co} h} \tag{30}$$

where $T_{f,max}$ and T_m represent the maximum fuel temperature (i.e. the centreline temperature) and the bulk temperature of the coolant, respectively.

Radially-averaging the temperature profiles leads to:

$$T_{f,ave} = T_m + q' \times \left(R_{eff} - \frac{1}{8\pi k_f}\right) \tag{31}$$

and

$$T_{c,ave} = T_m + q' \times \left[\frac{1}{2\pi R_{co} h} + \frac{1}{4\pi k_c} - \frac{R_{ci}^2}{R_{co}^2 - R_{ci}^2} \frac{1}{2\pi k_c} \ln\left(\frac{R_{co}}{R_{ci}}\right)\right] \tag{32}$$

for the fuel pellet and the cladding, respectively.

In order to estimate the heat transfer coefficient (appearing in the expressions above) between the outer cladding and the coolant, the knowledge of the outer cladding temperature is also required. It could be demonstrated that this temperature has the following expression:

$$T_w = T_m + \frac{q'}{2\pi R_{co} h} \tag{33}$$

Basically, Eqs. (31)-(33) represent the system of equations to be solved in order to resolve at a given axial level the radially-averaged fuel temperature, the radially-averaged cladding temperature, and the wall temperature (i.e. outer cladding temperature).

Some of the quantities appearing in the equations above, such as the heat transfer coefficients and the thermal conductivities, can only be determined from experimental correlations, themselves dependent on the temperatures being searched for. The problem is thus a non-linear problem.

The following correlations were thus used:

- For the fuel pellet: the thermal conductivity was determined using Eqs. 2.10, 2.8 and 2.12 from [20] and for a burnup equal to 30 GWd/tHM.
- For the gap: the gap conductance (i.e. heat transfer coefficient) was determined by interpolation using the data in Fig. 8-22 from [18].
- For the cladding: the thermal conductivity was determined by interpolation using the data in Table 2.IV from [20].
- For the coolant: the heat transfer coefficient was determined using Chen's correlation given by Eqs. 19-29 to 12.32 in [18].

The above correlations were implemented using the radially-averaged temperatures of the fuel pellet and the cladding instead of their local values. This represents an approximation which is deemed reasonable for the present study.

The three balance equations given by Eqs. (31)-(33) can be written for each of the axial nodes along the height of the fuel assembly. The vector of unknown quantities can thus be expressed as $\left[\left\langle T_{f,ave}\right\rangle_1;...;\left\langle T_{f,ave}\right\rangle_N;\left\langle T_{c,ave}\right\rangle_1;...;\left\langle T_{c,ave}\right\rangle_N;T_{w,1};...;T_{w,N}\right]^T$.

e. Coupling strategies and solution procedures

Three solution strategies were implemented to solve the multi-physics problem described above:

- A technique based on each physics solved one at a time using classical solution procedures and on iterations between each solver until convergence is reached. In the following, this technique is referred to as *Operator Splitting coupling*.
- A technique based on each physics solved one at a time and on iterations between each solver until convergence is reached. Nevertheless, contrary to the Operator Splitting coupling highlighted above, each mono-physics problem is formulated as a non-linear problem solved by the JFNK method. In the following, this technique is referred to as *JNFK-per physics coupling*.
- A technique where the entire multi-physics problem is formulated as one single set of balance equations automatically resolving the interdependencies between all fields. In the following, this technique is referred to a *JNFK monolithic coupling*.

In order to allow for a fair comparison between the three solution strategies above, the same initial guess was used for all solution procedures. When multi-physics iterations were performed (i.e. for the Operator Splitting coupling and for the JFNK-per physics coupling), a maximum of 20 multi-physics iterations were allowed. The convergence criterion was based on relative residuals being smaller than 10^{-5} per physics (when multi-physics iterations were preformed) and for the entire multi-physics problem.

Operator Splitting coupling

The neutronic problem was formulated as a single set of balance equations equivalently written as a matrix equation as:

$$\mathbf{A}\mathbf{x}_m = k_m \mathbf{x}_m \tag{34}$$

where $\mathbf{x}_m$ is the eigenvector and k_m the eigenvalue of the associated matrix $\mathbf{A}$. This problem was solved iteratively using the power iteration method (without acceleration), which reads as [15], [21]:

$$\mathbf{x}_m^{(p)} = \frac{1}{k_m^{(p-1)}} \mathbf{A}\mathbf{x}_m^{(p-1)} \tag{35}$$

and

$$k_m^{(p)} = k_m^{(p-1)} \frac{\mathbf{x}_m^{(p-1),T} \cdot \mathbf{x}_m^{(p)}}{\mathbf{x}_m^{(p-1),T} \cdot \mathbf{x}_m^{(p-1)}} \tag{36}$$

where p represents the iteration number. Starting guesses of the eigenvector $\mathbf{x}_m^{(0)}$ and of the eigenvalue $k_m^{(0)}$ need to be provided to the algorithm. This algorithm converges to the fundamental eigenmode and the corresponding eigenvalue, which is the largest. Those thus represent the static flux and the effective multiplication factor of the system.

For the fluid dynamics, an iterative procedure was also used. From an assumed axial distribution of the pressure, the mass and enthalpy conservation equations were first solved together. The momentum balance equation was then used to recalculate the pressure distribution and the process was repeated until convergence on the pressure was obtained. Concerning the algorithm used for solving the mass and enthalpy conservation equations (with the pressure assumed to be known), the problem was solved from the inlet to the outlet of the fuel channel, and the set of equations was solved one node at a time. From known values of the velocities and void fraction at the bottom of a node, a non-linear problem was formulated in terms of the velocities and void fraction at the top of the node, and a non-linear solver was applied for each of these single node problems. The non-linear solver used in MATLAB for that purpose was the `trust-region-dogleg` method (see MATLAB reference manual for `fsolve` [22]).

For the heat transfer problem, an iterative scheme was also used. From a known distribution of the axial profiles in radially-averaged fuel temperature, radially-averaged cladding temperatures, and outer cladding temperature, the various correlations appearing in the heat transfer problem were updated, and new temperature distributions were calculated using Eqs. (31)-(33). The process was repeated until convergence was achieved or a maximum number of iterations is reached.

JNFK-per physics coupling

The JFNK solution procedure was already explained in detail in Section 2. This method was applied to each of the mono-physics problems sequentially. When a given physics problem was computed, the fields from the other physics were frozen to their previous estimate. Iterations were thus performed until convergence was achieved or a maximum number of (outer) iterations reached.

Concerning the implementation details, an inexact Newton method was used, with a convergence criterion varying as the norm of the residuals. In addition, preconditioning of the problem was also tested. When used, two types of preconditioners were implemented:

- A preconditioner based on a numerical estimation of the actual Jacobian, referred to in this report as *numerical Jacobian*.
- A preconditioner based on a first-order approximation of the corresponding balance equations. In addition, for the fluid dynamics problem, the actual balance equations were first simplified by assuming equal velocities between the liquid and vapour phases. In such a case, the set of balance equations results in the Homogeneous Equilibrium Model (HEM) [18], [19]. In addition, the two-phase friction factors were kept equal to their steady-state values. This preconditioner is referred to as *analytical Jacobian* in this report. Although developing such an analytical Jacobian is by far one of the most demanding tasks in the implementation procedure, the resulting linearized balance equations are not presented in this report for the sake of brevity.

JNFK monolithic coupling

The JFNK solution procedure was already explained in detail in Section 2. Unlike the JNFK-per physics coupling, the balance equations were re-formulated in one single equivalent set of balance equations containing all the cross-dependencies between the various physics. An inexact Newton was also used and when a preconditioner was used, two types of preconditioning were tested: a preconditioning based on a numerical estimation of the actual Jacobian (referred to a *numerical Jacobian*) and a preconditioning based on a first-order approximation of the balance equations, and the use of the HEM for the fluid dynamics problem (preconditioning referred to as *analytical Jacobian*). In addition to the approximations already listed above in the JFNK per physics coupling for the analytical Jacobian, the scaling factor of the power density to the actual power level was kept to its steady-state value.

4. Comparisons between the various coupling alternatives

In order to allow for a fair comparison between the various solution procedures, the same initial starting guess was used. This initial guess is defined as follows:

- Flat axial pressure distribution equal to the outlet pressure.
- Velocity of the vapour phase assumed to be equal to twice the velocity of the liquid phase along the entire height of the channel.
- Flat void fraction distribution equal to 35%.
- Velocity of the liquid phase estimated by keeping the mass flux equal to its inlet value, with the axial distributions of the void fraction and velocity of the vapour phase as given above.
- Flat axial distributions of both the fast and thermal neutron flux, both having the same amplitude.
- Effective multiplication factor set to 1.5.
- Flat axial distributions of the radially-averaged fuel temperature, of the radially-averaged cladding temperature, and of the outer cladding temperature, all equal to the saturation temperature.

a. Results for Operator Splitting coupling

Calculations were first performed by iterating between the three solvers (neutronics, fluid dynamics, and heat transfer solvers) in a sequential manner, starting with the neutronics solver, followed by the fluid dynamics solver, and finally the heat transfer solver. In the following figures, the number of iterations represent the cumulative number of inner iterations for each mono-physics solver.

Although each solver converged with its respective set of boundary conditions, no converged multi-physics solution could be found after 20 multi-physics iterations. This can be seen in Fig. 3 where the so-called *apparent* residuals for each solver is plotted (labelled "NK" for the neutron transport solver, "FLUID" for the fluid solver, "TEMP" for the heat transfer problem), together with the *actual* residuals for the multi-physics set of balance equations (labelled as "ALL"). The apparent residuals for a given solver are estimated by freezing the solution for the other two solvers at the beginning of the mono-physics iterations. As can be seen in this figure, one notices that each solver converges to the desired convergence criteria.

Nevertheless, when looking at the actual residuals in Fig. 4, i.e. the residuals when the inter-dependences between the various sets of equations across the three solvers are considered, one notices that the desired convergence criteria are never met. The update of a mono-physics field leads to an increase of the residuals of the other two mono-physics fields. The overall residuals for the entire multi-physic solution (labelled as "ALL" in all figures) stagnate between 1 and 10. It can also be noticed from Fig. 4 that the heat transfer solver seems to be responsible for this stagnation, i.e. the actual residuals of the heat transfer solver is far larger

compared to the actual residuals for the neutronics and fluid dynamics solvers during the multi-physics updates.

In addition, it can be noticed from Fig. 5 that the multi-physic solutions are actually oscillating between two situations: a bottom-peaked neutron flux solution and a top-peaked neutron flux solution. This oscillatory behaviour in the multi-physics iterations is typical of light water reactors, and is representative of the strong feedback existing in the macroscopic data from coolant density and fuel temperature [2].

It was thus decided to apply a damping factor in the neutronic solution: when a new neutronic solution was computed, this solution was combined with the previous converged (mono-physics) neutronic solution, before being used in subsequent multi-physics updates, as follows:

$$\begin{aligned}&\left[\phi_{1,1};...;\phi_{1,N};\phi_{2,1};...;\phi_{2,N};k_{eff}\right]^{T,\text{next multi-physic iteration}}\\&=\theta\times\left[\phi_{1,1};...;\phi_{1,N};\phi_{2,1};...;\phi_{2,N};k_{eff}\right]^{T,\text{current mono-physic iteration}}\\&+\left(1-\theta\right)\times\left[\phi_{1,1};...;\phi_{1,N};\phi_{2,1};...;\phi_{2,N};k_{eff}\right]^{T,\text{past multi-physic iteration}}\end{aligned}\tag{37}$$

with $\theta = 0.5$. The results when a damping in the neutronic solution was applied can be seen in Fig. 6 for the apparent residuals and in Fig. 7 for the actual residuals. Although the behaviour of each mono-physics solver is in essence identical to the behaviour when no damping is applied, one notices that the multi-physics solution slowly converges to the desired convergence criteria.

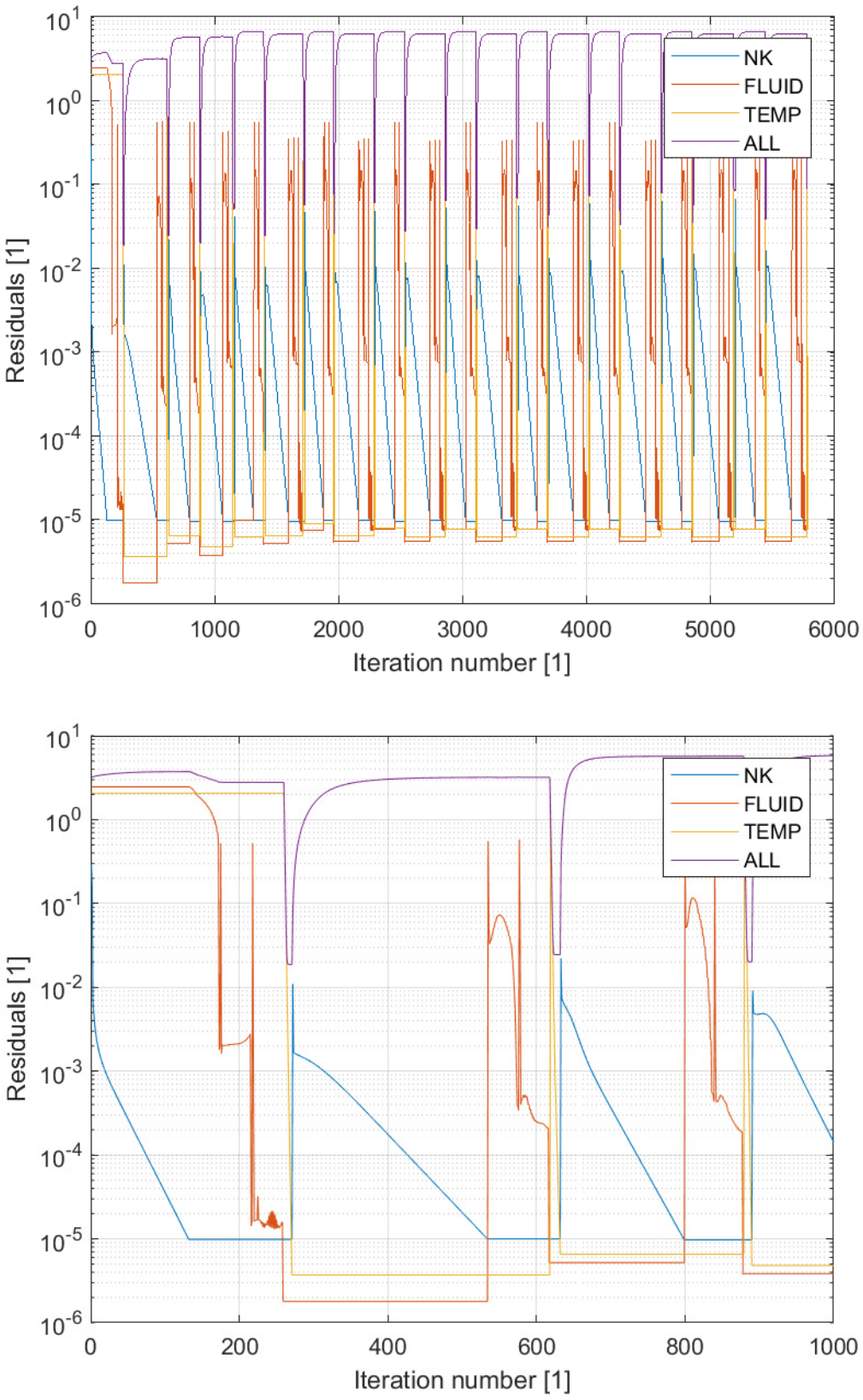

Fig. 3 Apparent residuals during the mono-physics and multi-physics iterations (all iterations given in the upper figure, only 1000 first iterations given in the lower figure).

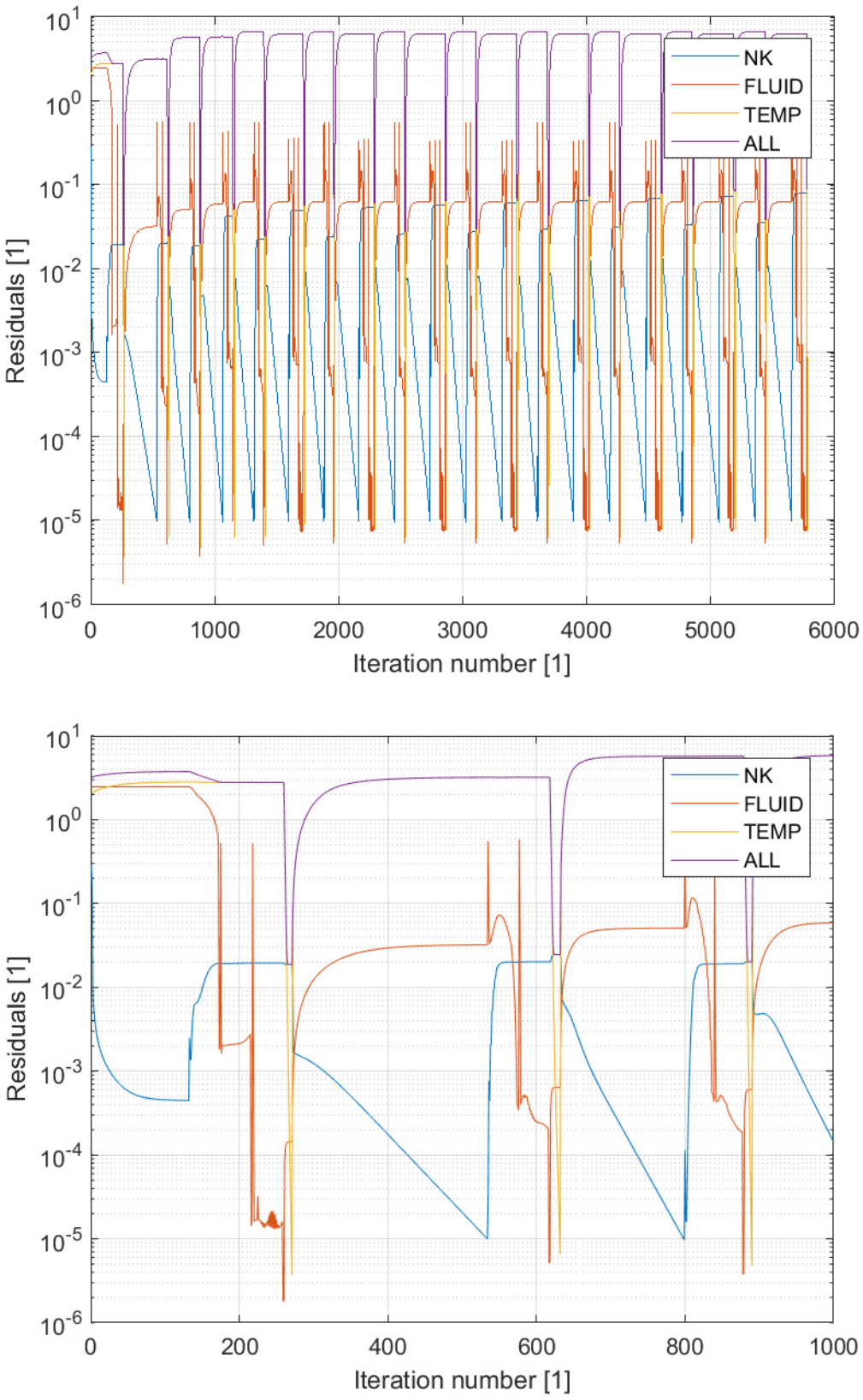

Fig. 4 Actual residuals during the mono-physics and multi-physics iterations (all iterations given in the upper figure, only 1000 first iterations given in the lower figure).

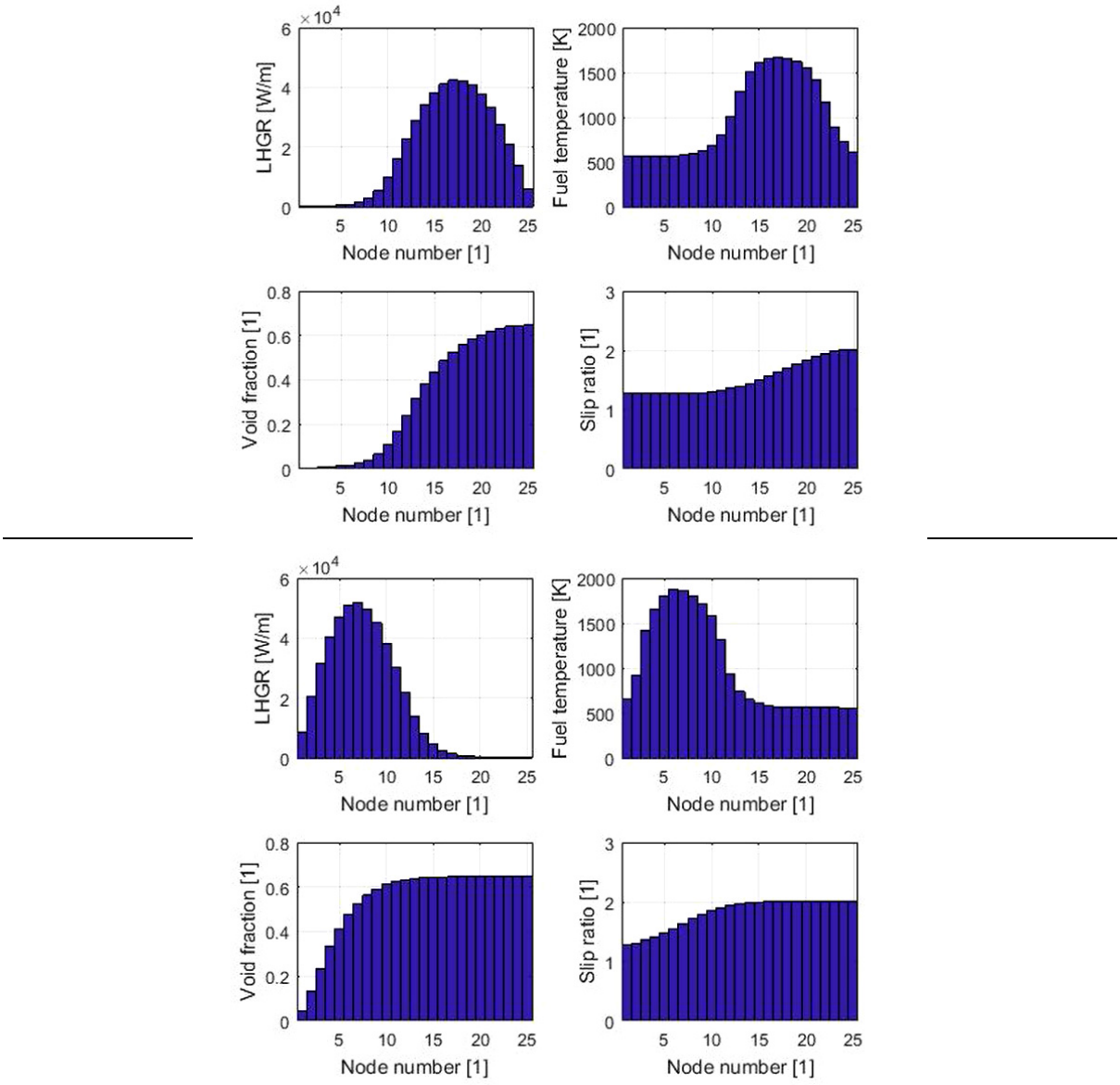

Fig. 5 Axial distributions of some representative quantities at the multi-physics iteration #19 (upper figure) and at the multi-physics iteration #20 (lower figure).

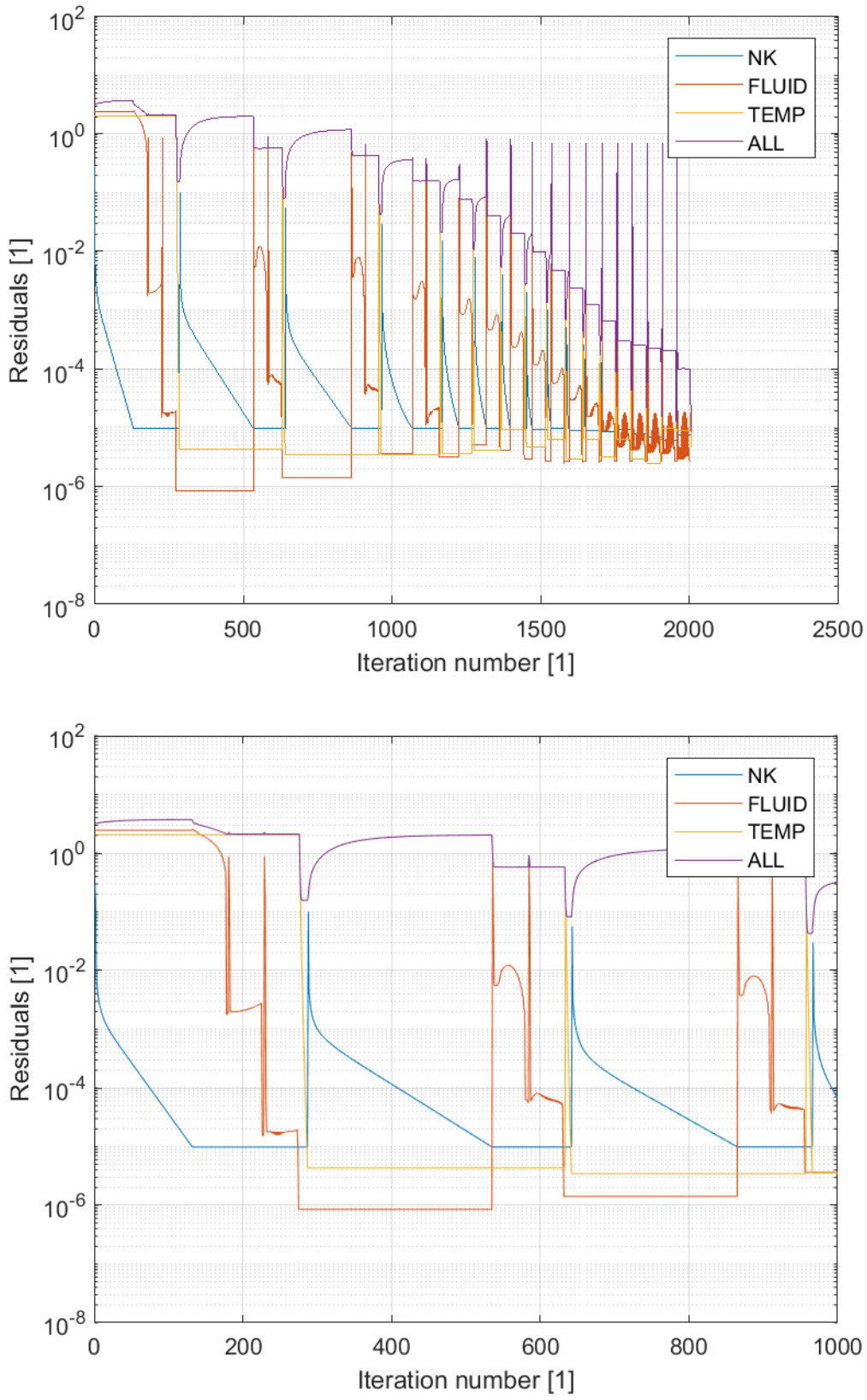

Fig. 6 Apparent residuals during the mono-physics and multi-physics iterations when damping in the neutronic solution is used (all iterations given in the upper figure, only 1000 first iterations given in the lower figure).

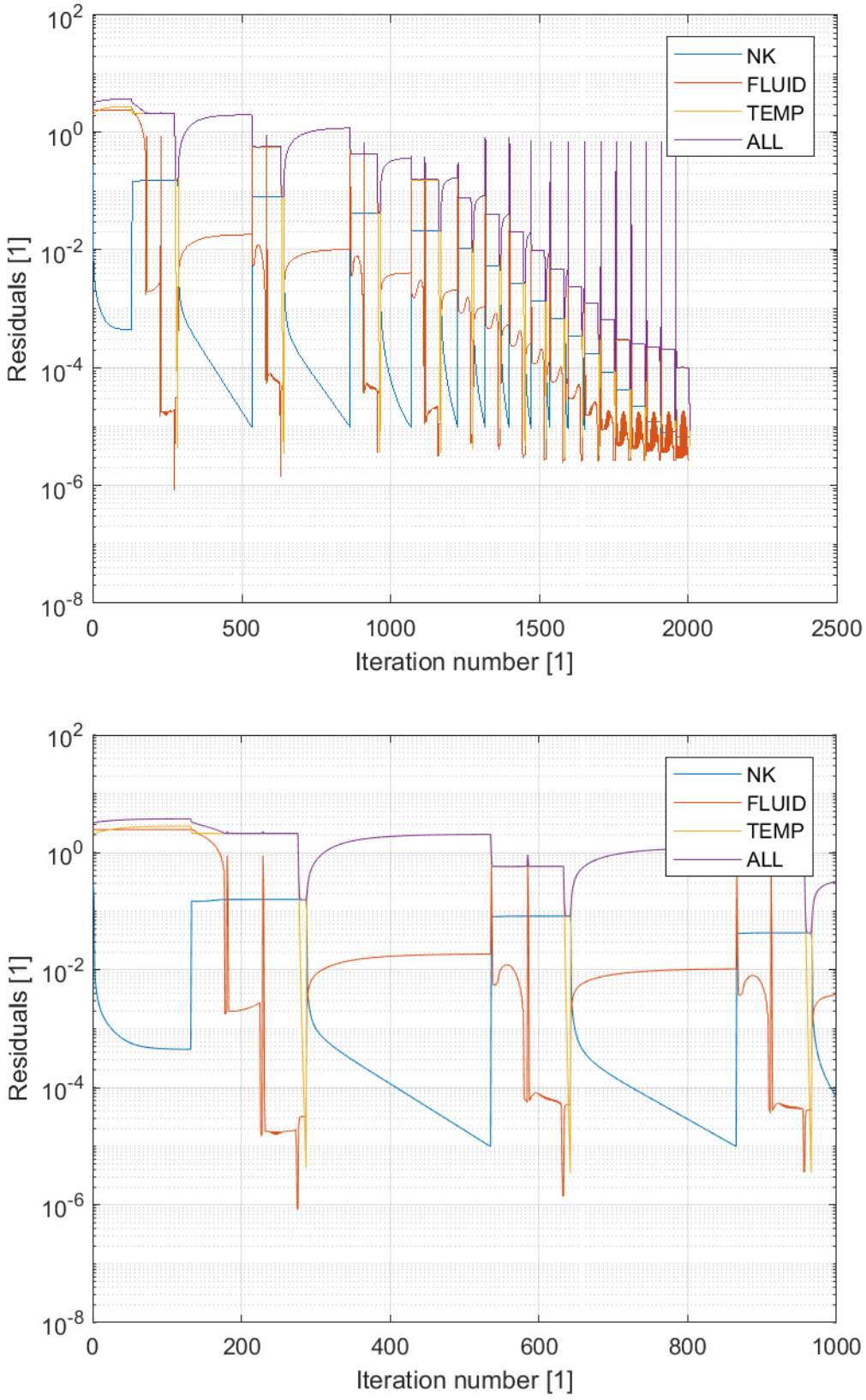

Fig. 7 Actual residuals during the mono-physics and multi-physics iterations when damping in the neutronic solution is used (all iterations given in the upper figure, only 1000 first iterations given in the lower figure).

b. Results for Jacobian-Free Newton Krylov per physics coupling

In this Section, each of the single physics problems is solved using a JFNK technique, and iterations are performed between the solvers until convergence is reached at the desired tolerance level. The neutron transport problem is first solved, then the fluid dynamics problem, followed by the heat transfer problem, and the process is repeated until convergence or when a maximum number of iterations is reached. In the following figures, the number of iterations represent the number of cumulative number of Newton iterations for each mono-physics solver (the number of GMRES iterations is not given).

If no damping factor is applied and if no preconditioning is used, the solver cannot converge to any physical solution, with the GMRES solver failing at the fourth multi-physics iteration for estimating the neutronic solution, as can be seen in Fig. 8. The apparent and actual residuals are given in Fig. 9. Although very few multi-physics iterations were performed, one notices that the same behaviour as with the operator splitting coupling. Namely, although each mono-physics solver converges to the required tolerance, the multi-physics solution is far from converging, with the heat transfer problem mostly responsible for the large residuals observed.

If no damping is applied but a preconditioner using an analytical Jacobian is used, the GMRES solver again fails at the fourth multi-physics iteration for estimating the neutronic solution. As noticed in the previous case without preconditioning, an oscillatory behaviour in the neutronic solution is present. The last multi-physic iterates of the solution returned by the solver before failing are given in Fig. 10. The apparent and actual residuals are given in Fig. 11. In essence, the behaviour of the solver is identical to the case without preconditioning.

If damping of the neutronics solution (as given by (37)) is applied but no preconditioning used, the coupled solver converges very slowly to a physical solution, as can be noticed in Fig. 12 for the apparent residuals and in Fig. 13 for the actual residuals. The behaviour of the solver is equivalent to the operator splitting coupling, with the heat transfer solution mostly responsible for the large values of the residuals during the multi-physics iterations.

Finally, if damping of the neutronics solution (as given by (37)) is applied and an analytical preconditioning is used, the coupled solver converges very slowly to a physical solution. Slightly less iterations are nevertheless required compared to the case where no preconditioning is applied. The apparent residuals are represented in Fig. 14 and the actual residuals are represented in Fig. 15. No significant differences compared to the case where no preconditioning is used can be noticed.

One thus concludes that the ability of the solver to converge to a physical solution is entirely governed by the damping of neutronic solution during the multi-physics updates.

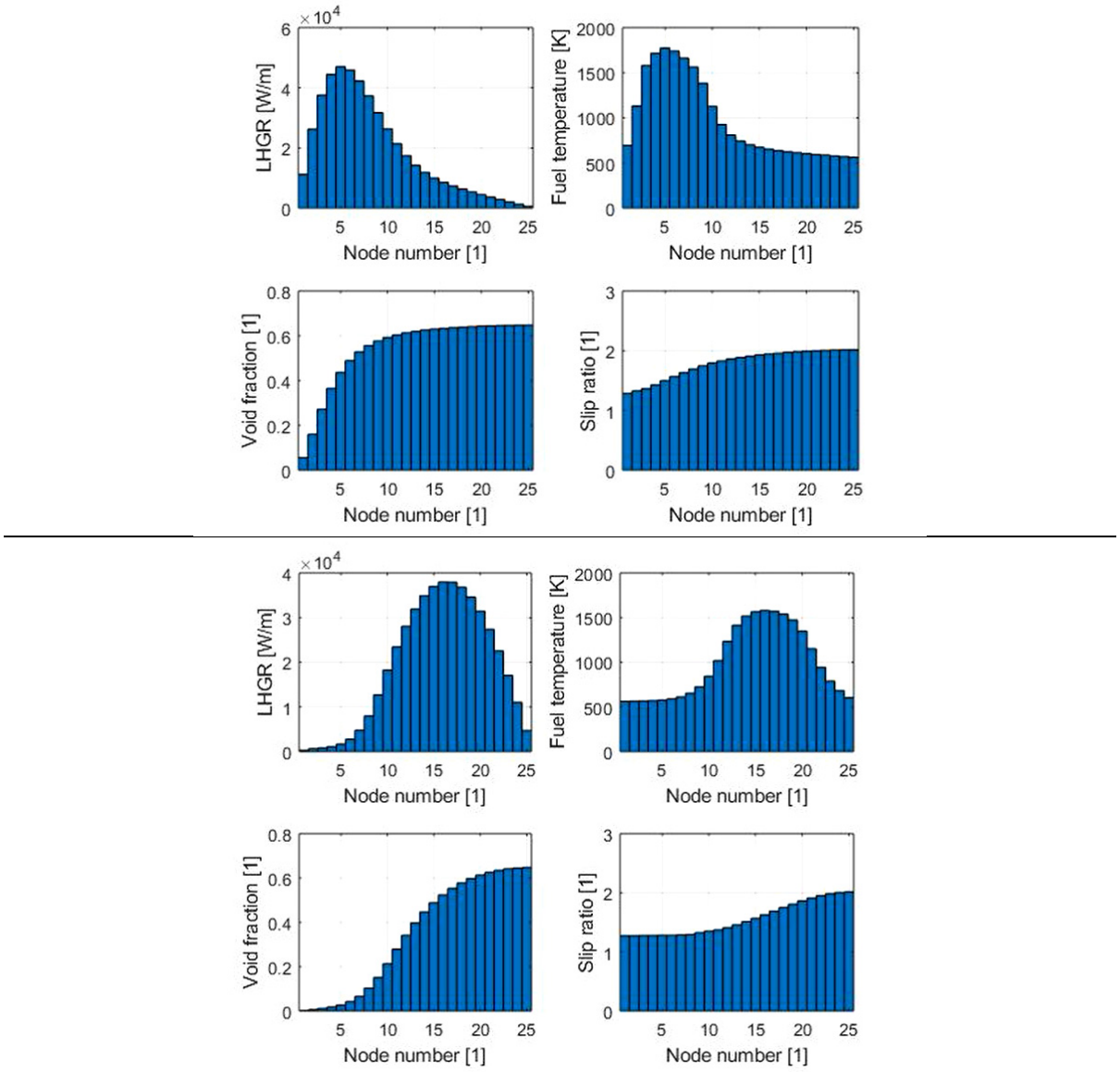

Fig. 8 Axial distributions of some representative quantities at the multi-physics iteration #2 (upper figure) and at the multi-physic iteration #3 (lower figure).

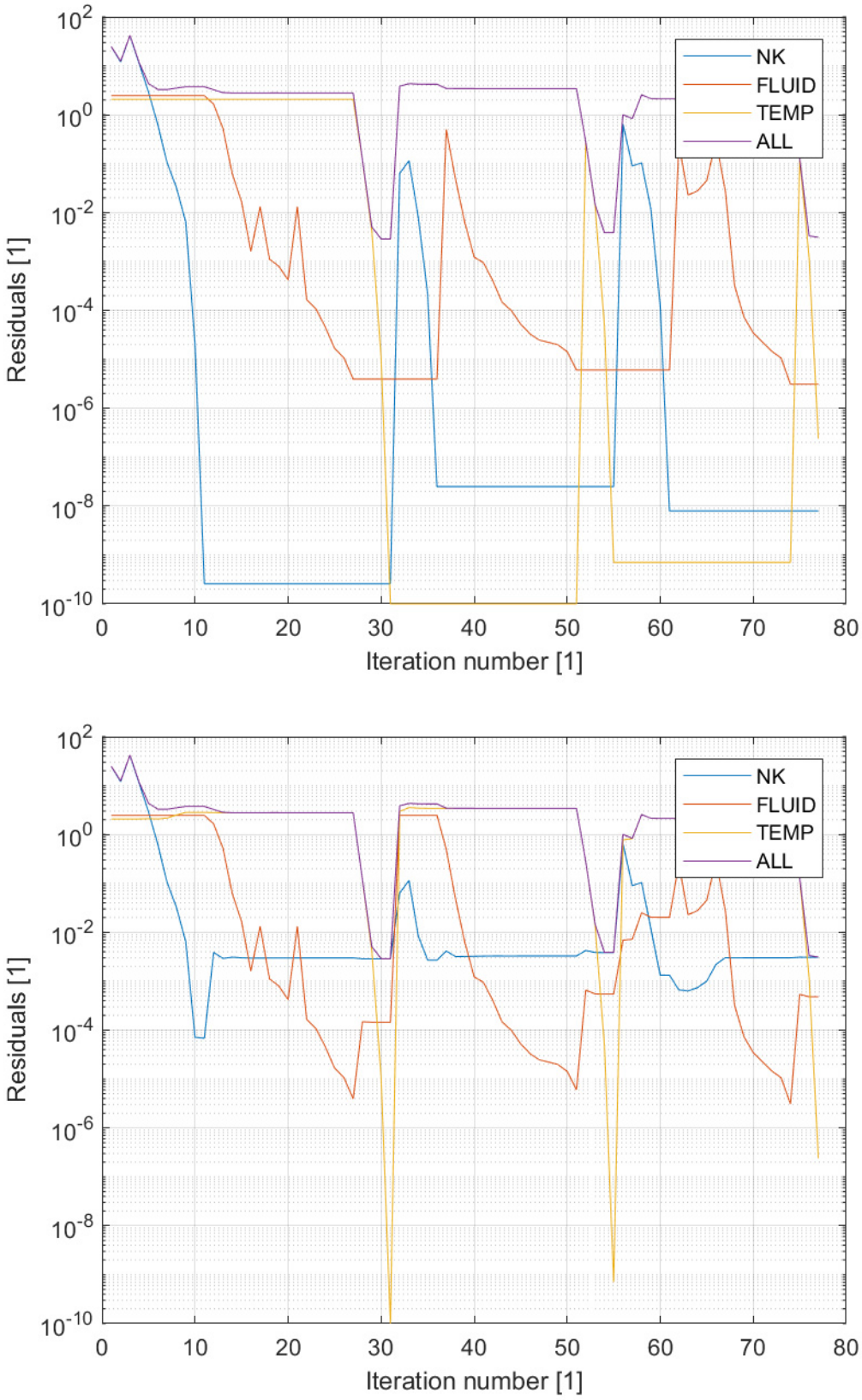

Fig. 9 Apparent residuals (upper figure) and actual residuals (lower figure) during the mono-physics and multi-physics iterations.

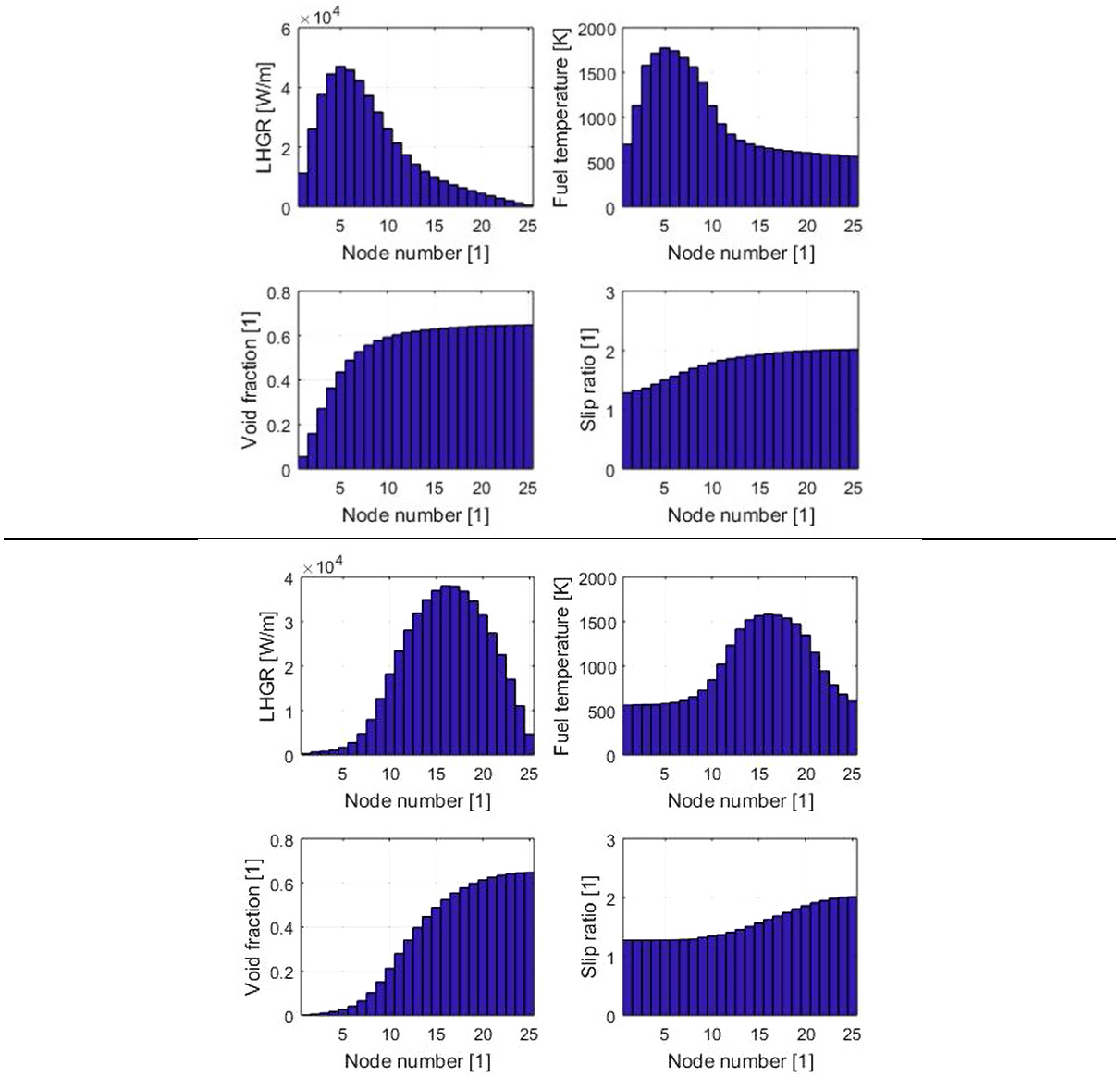

Fig. 10 Axial distributions of some representative quantities at the multi-physics iteration #2 (upper figure) and at the multi-physic iteration #3 (lower figure).

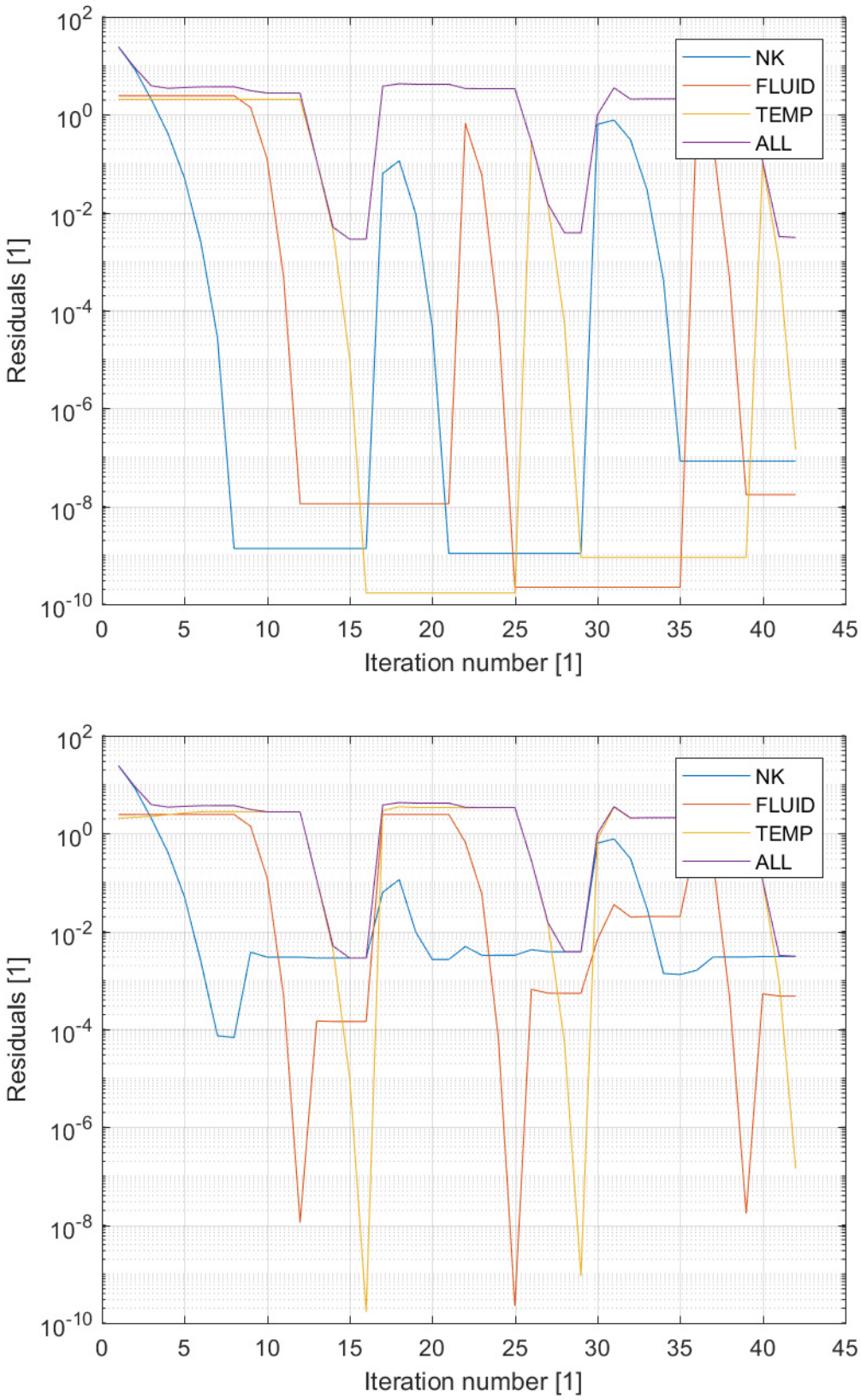

Fig. 11 Apparent residuals (upper figure) and actual residuals (lower figure) during the mono-physics and multi-physics iterations.

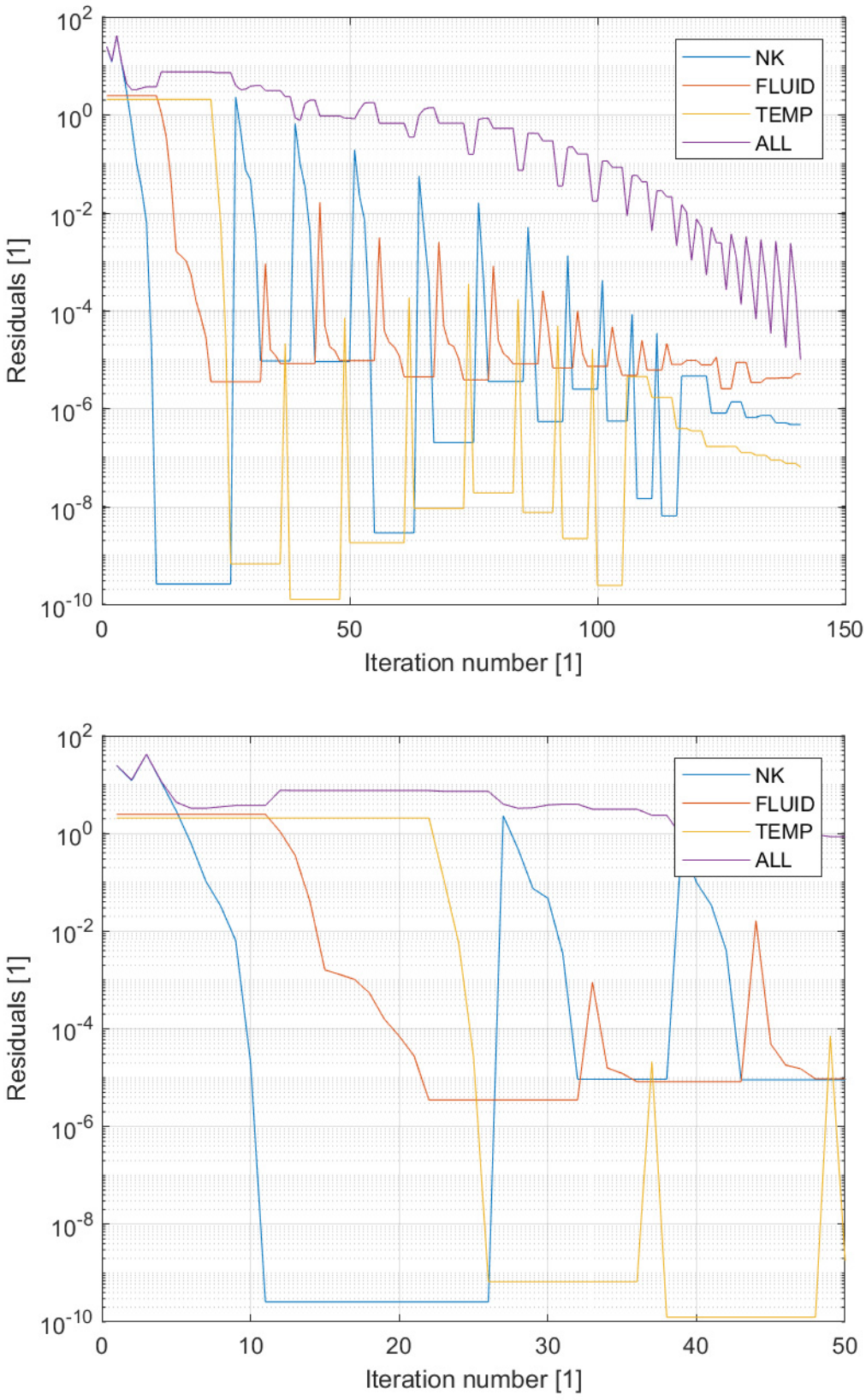

Fig. 12 Apparent residuals during the mono-physics and multi-physics iterations when damping in the neutronic solution is used (all iterations given in the upper figure, only 50 first iterations given in the lower figure).

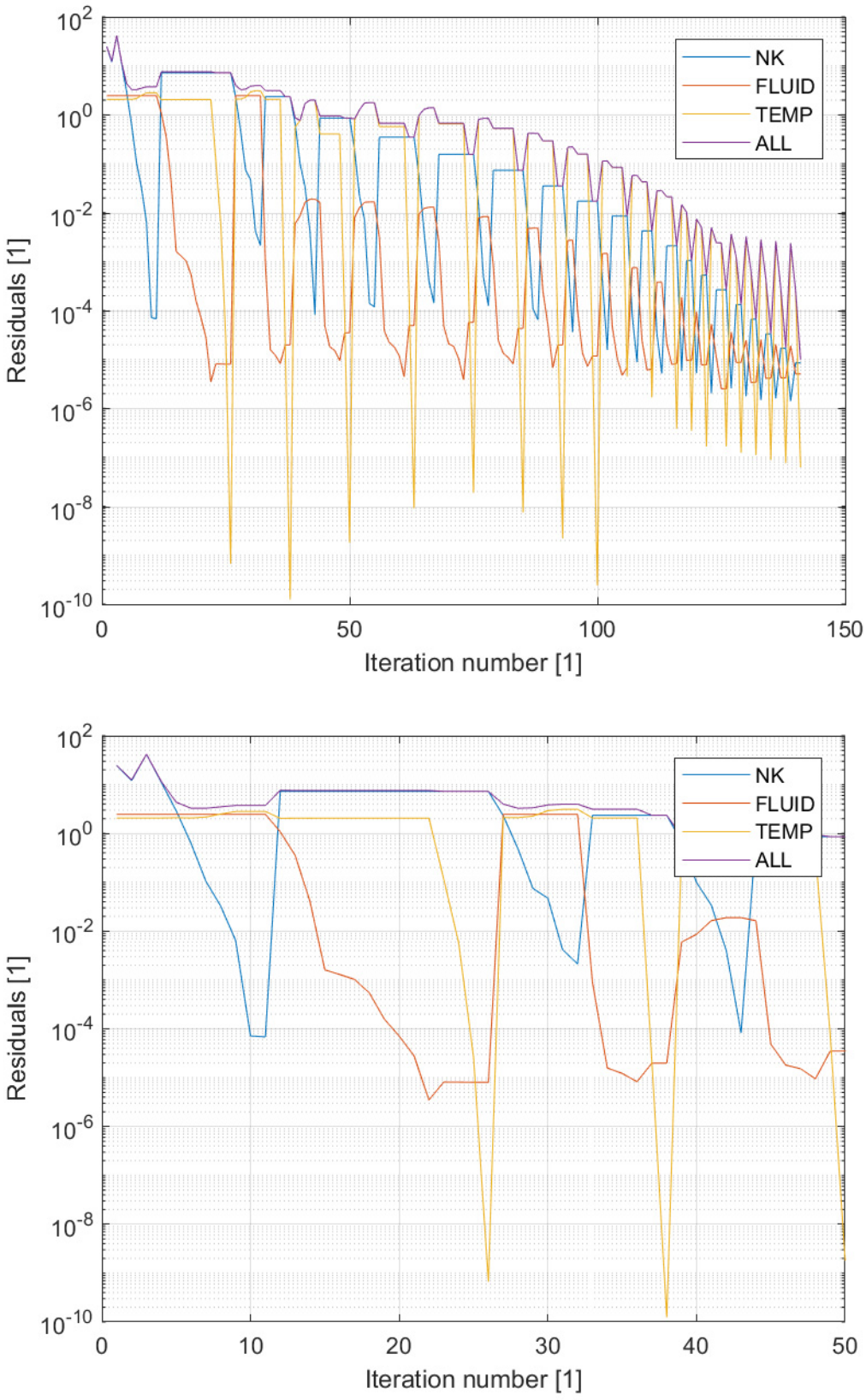

Fig. 13 Actual residuals during the mono-physics and multi-physics iterations when damping in the neutronic solution is used (all iterations given in the upper figure, only 50 first iterations given in the lower figure).

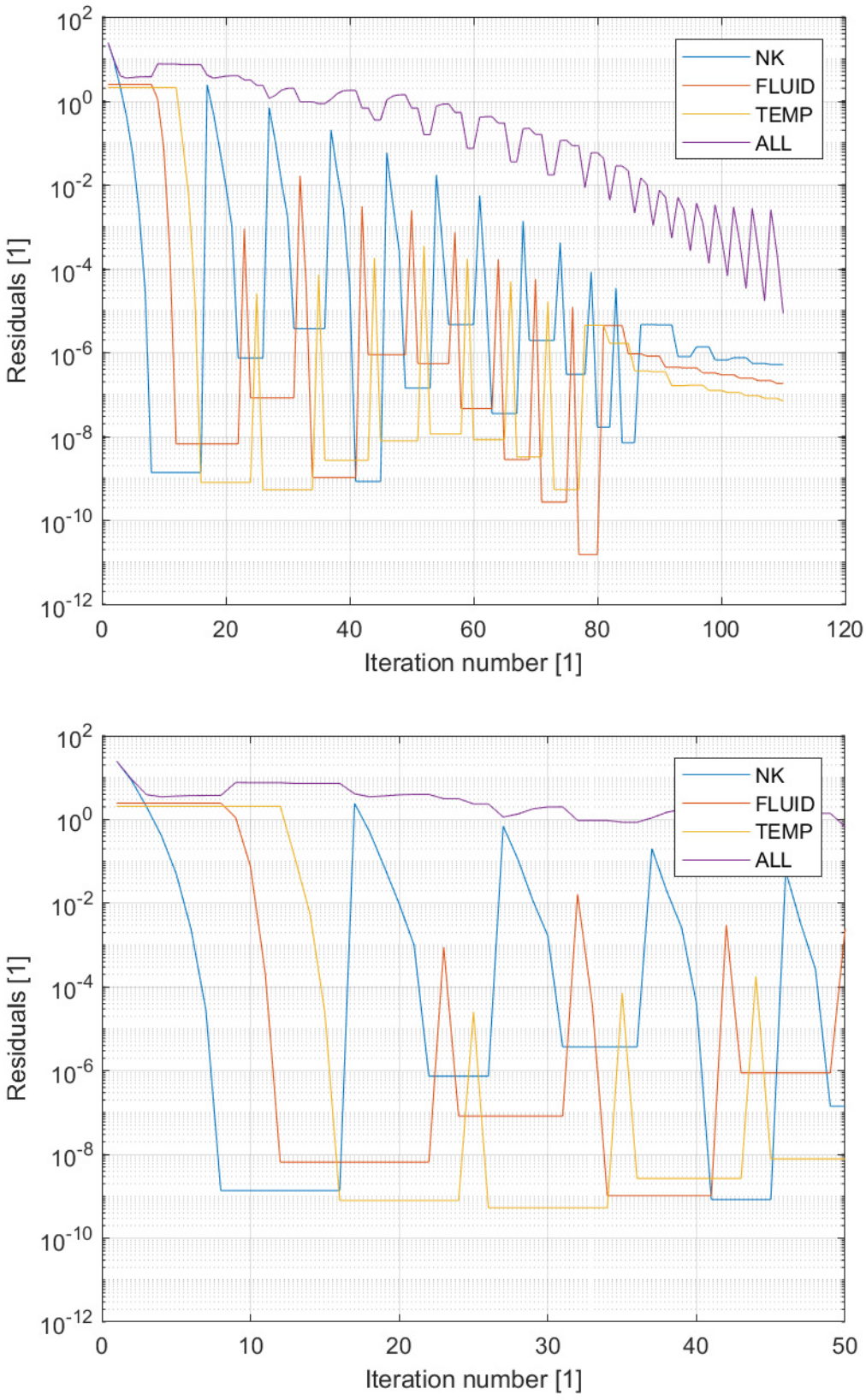

Fig. 14 Apparent residuals during the mono-physics and multi-physics iterations when damping in the neutronic solution and preconditioning are used (all iterations given in the upper figure, only 50 first iterations given in the lower figure).

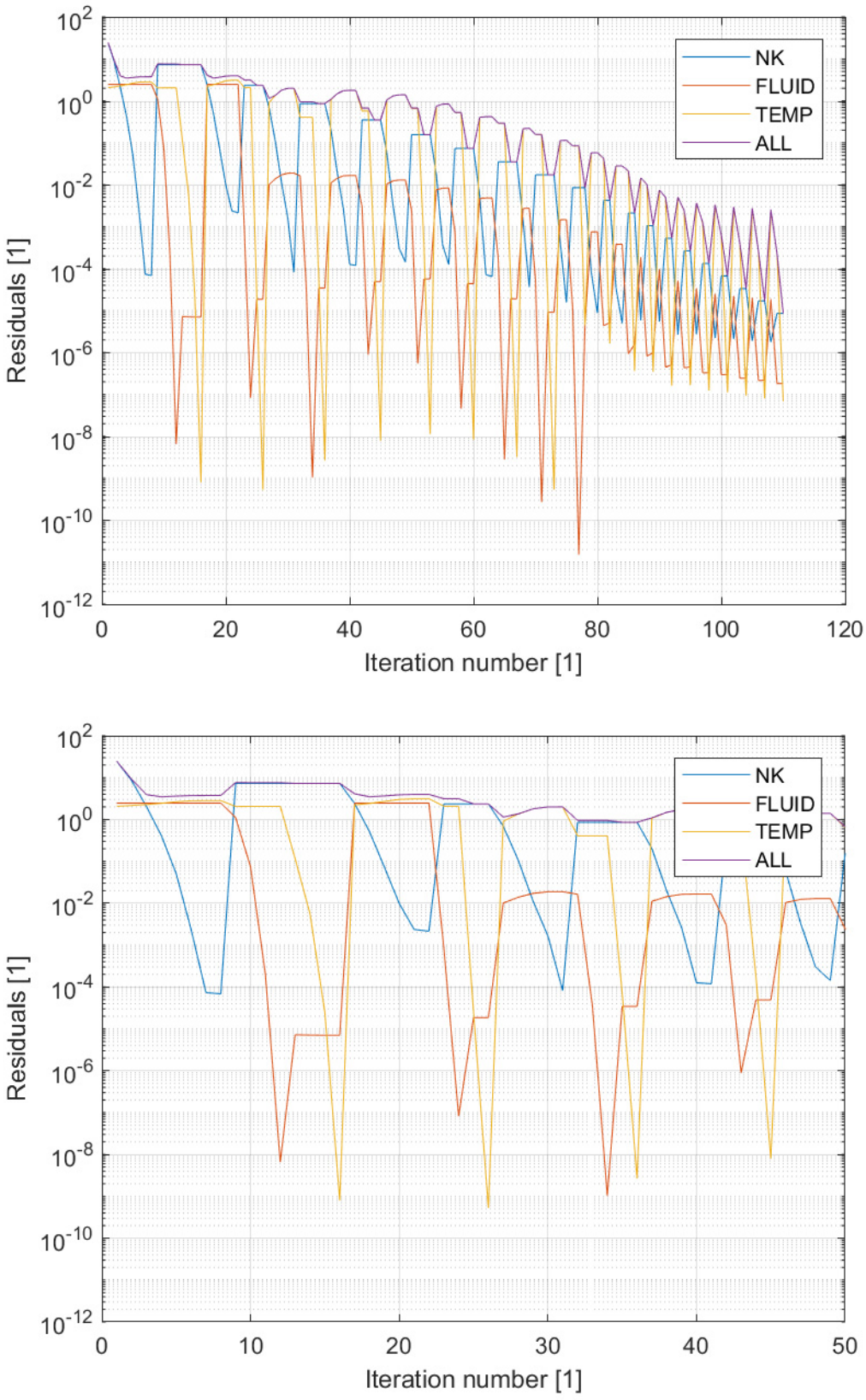

Fig. 15 Actual residuals during the mono-physics and multi-physics iterations when damping in the neutronic solution and preconditioning are used (all iterations given in the upper figure, only 50 first iterations given in the lower figure).

c. Results for Jacobian-Free Newton Krylov monolithic coupling

In this Section, the entire multi-physic problem is solved simultaneously by resolving all cross-dependencies between the various physics. Due to the non-linear nature of the problem at hand, the JFNK method is used for solving the set of multi-physics equations.

In the JFNK per physics coupling approach, whereas preconditioning was found to be lead to slightly faster convergence, damping in the neutronic solution was a necessity to avoid the appearance of numerical oscillations.

In the JFNK monolithic coupling, early tests demonstrated the necessity to use preconditioning. Although each of the mono-physics problem can be solved separately from each other without preconditioning, the entire multi-physics problem has a much larger condition number due to the different nature of the balance equations thus assembled in a monolithic approach. Preconditioning leads to a lower condition number and results in an increased convergence rate.

Fig. 16 represents the actual residuals when the analytical Jacobian is used. Since the entire multi-physics problem is solved at once, the apparent residuals are in the present case identical to the actual residuals. As can be seen in this figure, the solver convergences to the require tolerance in 15 iterations. As noticed for the other types of coupling methods earlier detailed, the residuals in the heat transfer problem are responsible for most of the residuals in the entire multi-physics problem. It should also be emphasized that the solver seems to go through some “difficult” first iterations (noticed in the temperature distributions essentially), during which the computed solution does not resemble the expected physical solution. Other tests (not detailed in this report) demonstrated that the solver might not always be able to find a physical solution depending on the initial guess used. In order to guarantee a solver converging whatever initial guess is applied, some intermediate steps to force the monolithic JFNK approach to find a physical solution is desired – see Section 6.

Fig. 17 represents the actual residuals when the numerical Jacobian is used instead. Compared to the case where an analytical Jacobian is used, the solver converges in 8 iterations only. The first “difficult” iterations disappear when using the numerical Jacobian. Some further analysis revealed that the first “difficult” iterations can be partially removed when using an analytical Jacobian for which the cross-dependencies in the temperature fields coming the neutronic solution are not considered. As earlier explained, the analytical Jacobian does not consider the effect of the normalization of the neutronic solution to a fixed power level. The corresponding part of the preconditioner describing the coupling from the neutron kinetics to the temperature solved is thus inaccurate. Turning off this part of the preconditioner leads to a solver converging in 10 iterations and for which the first “difficult” iterations are less pronounced.

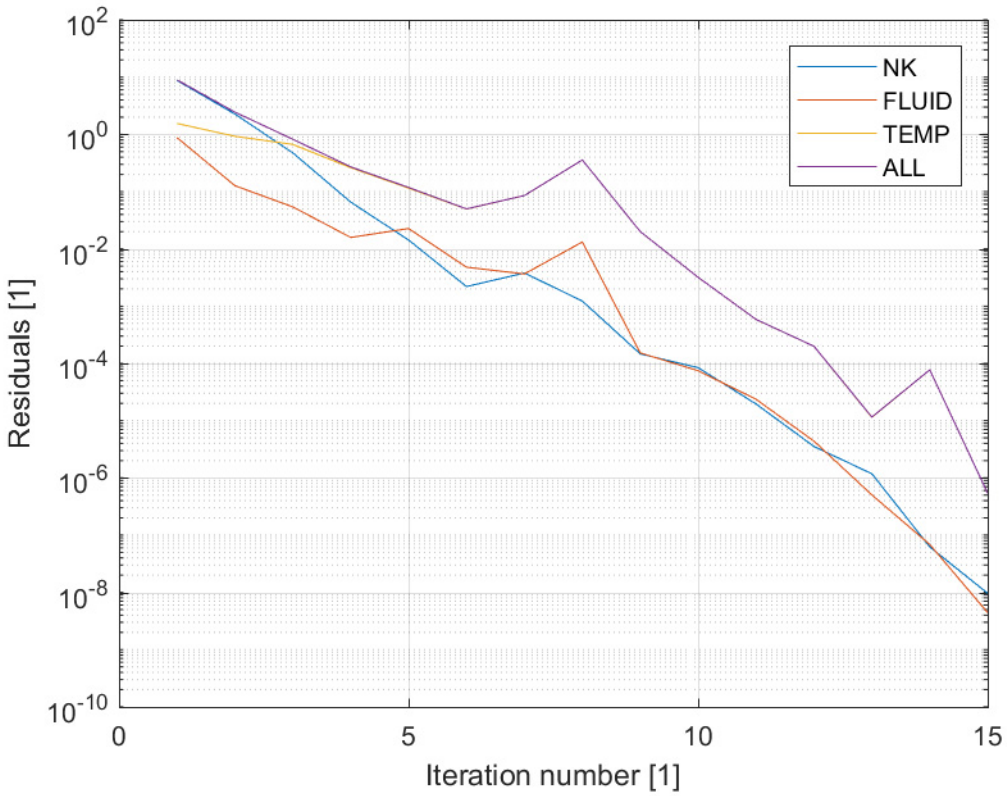

Fig. 16 Actual residuals during multi-physics iterations when the analytical preconditioner is used.

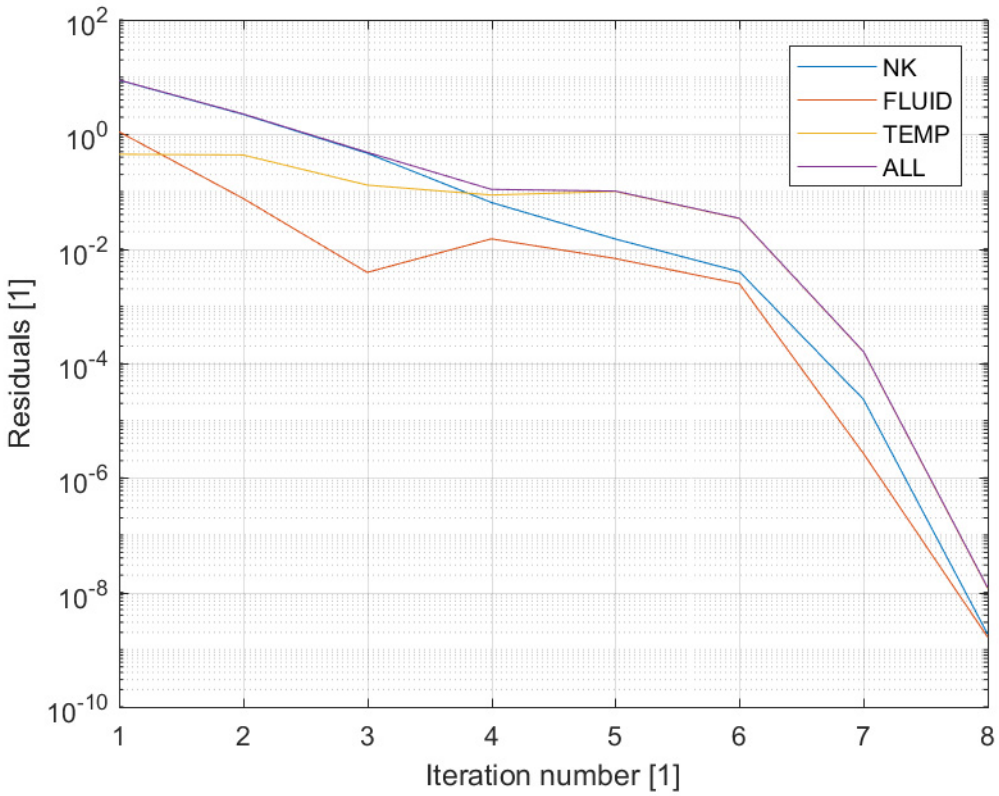

Fig. 17 Actual residuals during multi-physics iterations when the numerical preconditioner is used.

d. Conclusions

When solving a multi-physics problem in a segregated manner, i.e. by iterating between mono-physics solvers until convergence, damping of the neutronic solution is a necessity. This is the result of the strong feedback mechanism existing between coolant density/fuel temperature and nuclear macroscopic data.

The use of a JNFK per physics approach, although leading to slightly less multi-physics iterations (especially when preconditioning is used), comes at the expense of the necessity to reformulate each mono-physics problem into a set of balance equations with a zero-right-hand side, i.e. each mono-physics solver needs to be modified or rewritten. Considering the accumulated V&V work on legacy mono-physics codes, such code modifications for making use of a JFNK per physics approach are not worth the effort.

On the other hand, using a monolithic JFNK approach to solve simultaneously the entire multi-physics problem allows avoiding the use of any damping and leads to faster convergence, if a proper preconditioner is used. Although building upon existing codes and

solution algorithms is possible, a monolithic JFNK approach requires the development of a new software where the set of balance equations for all physics is present.

5. Investigation of the effect of preconditioning

The tests performed in this Section were performed with slightly different implementation options compared to the ones used in Section 4. The most notable differences are:

- A maximum of 50 multi-physic iterations were allowed.
- The convergence criterion was based on relative residuals being smaller than 10^{-6} for the entire multi-physics problem.
- An exact Newton method was used, with a convergence criterion set to 10^{-8}.
- The initial guess was defined as follows:
    - Flat axial pressure distribution equal to the outlet pressure.
    - Void fraction having a sinusoidal shape varying between 0% at the inlet to 70% at the outlet.
    - Velocity of the vapour phase assumed to be equal to twice the velocity of the liquid phase along the entire height of the channel.
    - Velocity of the liquid phase estimated by keeping the mass flux equal to its inlet value, with the axial distributions of the void fraction and velocity of the vapour phase as given above.
    - Flat axial distributions of both the fast and thermal neutron flux. The thermal flux was assumed to be 10 times smaller than the fast flux.
    - Effective multiplication factor set to 1.0.
    - Flat axial distributions of the radially-averaged cladding temperature, and of the outer cladding temperature, all equal to the saturation temperature.
    - Flat axial distributions of the radially-averaged fuel temperature equal to two times the saturation temperature.
- "Regularized" drift-flux correlations were used, i.e. a smoothing of the correlations used for the drift-flux model at $\left\langle \underline{\alpha} \right\rangle = 0.15$ and at $\left\langle \underline{\alpha} \right\rangle = 0.25$ was carried out.

a. Introduction

The design of an efficient preconditioner is one of the key aspects in the monolithic JFNK approach. The best possible preconditioner is the Jacobian of the system of equations itself, which could be estimated by numerically differentiating the set of equations with respect to each of the primary variables solved for. Even if one could use a first-order approximation for making those evaluations, a numerical Jacobian is of little use when trying to solve the set of equations in a Jacobian-free manner. The purpose of the JFNK method is to avoid the actual computation of the Jacobian traditionally required in the Newton method. Such a task is demanding from a CPU viewpoint, since it requires the computation of the first-order derivatives of each balance equation with respect to each of the primary variables. Using an analytical preconditioner thus represents an interesting alternative. Nevertheless, the required efforts in developing such an analytical Jacobian are far bigger than developing the set of equations and associated models to be solved by the JFNK approach. The purpose of this

section is to investigate how to develop efficient preconditioners for the BWR set-up considered in this study.

b. Understanding the structure of the preconditioner

If one assembles the vector of the primary variables in the following manner:

$$\mathbf{x} = \left[\mathbf{x}^{NK}; \mathbf{x}^{FLUID}; \mathbf{x}^{TEMP}\right]^T \tag{38}$$

with

$$\mathbf{x}^{NK} = \left[\phi_{1,1}; ...; \phi_{1,N}; \phi_{2,1}; ...; \phi_{2,N}; k_{eff}\right] \tag{39}$$

$$\mathbf{x}^{FLUID} = \left[\left\{\underline{\alpha}\right\}_{1+1/2}; ...; \left\{\underline{\alpha}\right\}_{N+1/2}; \left\{v_l\right\}_{1+1/2}; ...; \left\{v_l\right\}_{N+1/2}; \left\{v_v\right\}_{1+1/2}; ...; \left\{\overline{v}_v\right\}_{N+1/2}; \left\{\hat{P}\right\}_{1/2}; ...; \left\{\hat{P}\right\}_{N-1/2}\right] \tag{40}$$

$$\mathbf{x}^{TEMP} = \left[\left\langle T_{f,ave}\right\rangle_1; ...; \left\langle T_{f,ave}\right\rangle_N; \left\langle T_{c,ave}\right\rangle_1; ...; \left\langle T_{c,ave}\right\rangle_N; T_{w,1}; ...; T_{w,N}\right] \tag{41}$$

the structure of the resulting Jacobian looks as depicted in Fig. 18. The Jacobian represented in this figure was estimating by first-order differentiating each of the balance equations with respect to each of the chosen primary variables.

The Jacobian is essentially a sparse matrix. It is made of three main diagonal blocks and six off-diagonal blocks. The diagonal blocks essentially represent each of the mono-physics problems: “NK to NK” for neutron transport; “FLUID to FLUID” for fluid dynamics; and “TEMP to TEMP” for heat transfer. The off-diagonal blocks represent the coupling existing between the various physics: “NK to FLUID” and “FLUID to NK” for the coupling from neutron transport to fluid dynamics and vice versa, respectively; “NK to TEMP” and “TEMP to NK” for the coupling from neutron transport to heat transfer and vice versa, respectively; and “FLUID to TEMP” and “TEMP to FLUID” for the coupling from fluid dynamics to heat transfer and vice versa, respectively.

The Jacobian is primarily a sparse matrix. The dense blocks appearing in the Jacobian come from the normalization of the power density to a fixed power level for the entire channel. Each primary variable perturbing the estimation of the power density in one axial node has thus an effect on the entire length of the heated channel.

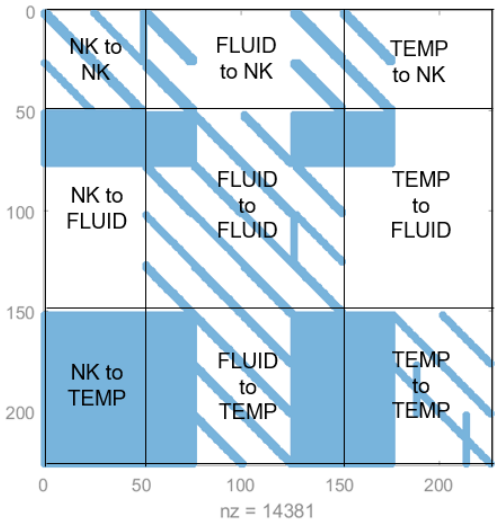

Fig. 18 Structure of the Jacobian in the monolithic multi-physics problem.

c. Effect of partial preconditioning

Although mostly sparse, the estimation of each on the non-zero terms of the Jacobian in an analytical manner represents a major effort, far bigger than developing a monolithic JFNK approach and formulating the corresponding residuals.

The essence of preconditioning is to change the condition number of the system being solved. This is achieved by modifying the original problem formulated as:

$$\mathbf{J}\left(\mathbf{x}^k\right)\delta\mathbf{x}^k = -\mathbf{F}\left(\mathbf{x}^k\right) \tag{42}$$

by the following problem (right preconditioning) [23]:

$$\left[\mathbf{J}\left(\mathbf{x}^k\right)\mathbf{P}^{-1}\left(\mathbf{x}^k\right)\right]\left[\mathbf{P}\left(\mathbf{x}^k\right)\delta\mathbf{x}^k\right] = -\mathbf{F}\left(\mathbf{x}^k\right) \tag{43}$$

where $\mathbf{P}$ is the preconditioning matrix. The effect of the preconditioning is to efficiently cluster the eigenvalues of the problem around unity. Equivalently, a preconditioner should be seen as a good enough approximation of the actual Jacobian, so that $\mathbf{J}\left(\mathbf{x}^k\right)\mathbf{P}^{-1}\left(\mathbf{x}^k\right) \approx \mathbf{I}$ where $\mathbf{I}$ is the identity matrix. In these conditions, the number of iterations necessary to reach the solution to the desired convergence criteria can be greatly reduced. Because of the multi-physics nature of the problem at hand, it is very likely that some of the eigenvalues are already clustered. A preconditioning related to these eigenvalues is thus unnecessary.

In the following, the effect of partially conditioning the actual problem using the numerical Jacobian is investigated, so that it is possible to identify the parts of the system of equations

that need to be preconditioned. For that purpose, the eigenvalues of the system are determined. If such eigenvalues are not clustered, a preconditioning related to these eigenvalues is thus tested using the corresponding parts of the Jacobian.

In Fig. 19, the effect of block-preconditioning each of the mono-physics problems is investigated, i.e. neglecting the cross-dependencies between the various physics. The eigenvalues of the actual Jacobian of the entire system are represented on the left figure and labelled as "Jac", together with the eigenvalues of each of the mono-physics problem. It can be noticed that only the eigenvalues related to fluid dynamics and neutron transport are not clustered. The middle figure gives the eigenvalues when the neutron transport, the fluid dynamics, and the heat transfer problems are separately preconditioned and when only neutron transport and the fluid dynamics problems are preconditioned. As can be seen, the effect of neglecting the preconditioning of the heat transfer problem seems to be negligible. This can also be noticed on the right figure, where the residuals are plotted as functions of the iteration number. Using a mono-physics block preconditioning greatly improves the convergence rate compared to non-preconditioning at all (for which the condition number is about 3.70×10^8). Nevertheless, not preconditioning the heat transfer problem does not seem to have any significant effect on the convergence rate. The condition numbers with heat transfer preconditioning included is 1.72×10^6, whereas it is 1.68×10^6 when excluded.

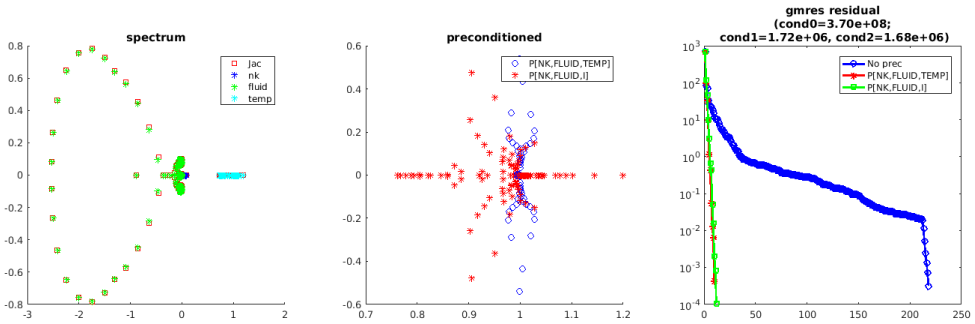

Fig. 19 Effect of preconditioning each of the physics separately.

It can thus be concluded that, in order to develop an efficient preconditioner, it is sufficient to precondition the neutron transport problem and the fluid dynamics problem separately, without taking the cross-dependencies between any mono-physics solver into account.

Although the design of a preconditioner for the neutron transport problem does not represent a major undertaking, due to the essentially linear nature of the governing equations, the design of a preconditioner for the fluid dynamics problem constitutes a challenge. This is due to the fact that the fluid dynamics problem is a strongly non-linear problem containing many interdependencies between the primary variables. In the following, we will investigate whether all the cross-dependencies need to be retained for efficiently preconditioning the fluid dynamics problem.

Fig. 20 investigates the effect of preconditioning each of the primary variables separately in the fluid dynamics solver. In this figure, the actual Jacobian of the fluid dynamics problem solely is labelled as "JF". As can be seen on the left figure, the eigenvalues associated to the void fraction, the liquid velocity, the vapour velocity, and the pressure are not clustered. Applying a mono-variable preconditioning leads to clustered eigenvalues, as seen in the middle figure. When looking at the convergence rate without preconditioning (with a condition number of 7.86×10^3) and with preconditioning (with a condition number of 7.51×10^3), one notices that a mono-variable preconditioning for the fluid dynamics solver increases the convergence rate, but as can be seen on the left figure, some other important eigenvalues in the actual Jacobian do not seem to be captured by a mono-variable preconditioner. This means that resolving some of the cross-dependencies seems necessary.

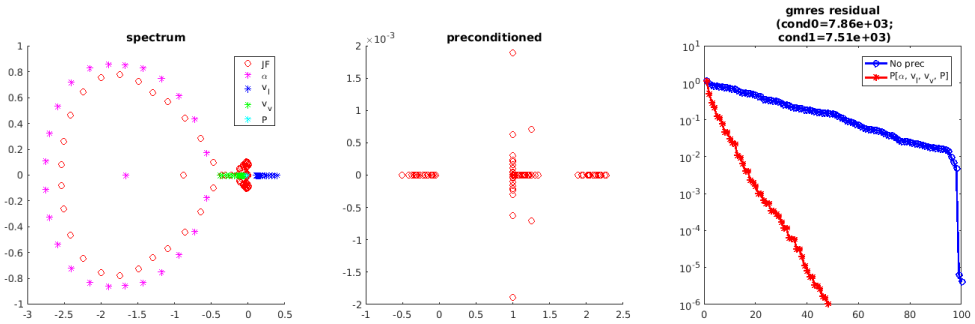

Fig. 20 Effect of preconditioning each of the fluid primary variables separately.

Several possibilities for resolving in the fluid dynamics the cross-dependencies between the primary variables were investigated:

(a) Void fraction and pressure treated separately, but interdependencies between phasic velocities taken into account – see Fig. 21.
(b) Interdependencies between the phasic velocities taken into account and interdependencies between void fraction and pressure taken into account – see Fig. 22.
(c) Void fraction treated separately and interdependencies between phasic velocities and pressure taken into account – see Fig. 23.
(d) Interdependencies between void fraction and phasic velocities taken into account and pressure treated separately – see Fig. 24.

For each of the figures, the eigenvalues of the actual Jacobian for the fluid dynamics problem solely are given on the left and labelled as "JF", together with the eigenvalues associated to the corresponding hypotheses (a, b, c or d). The eigenvalues of the preconditioned systems for each of the hypotheses are represented in the middle figures, whereas the convergence rate is depicted on the right figures. As can be seen in these figures, the three first alternatives lead to identical results, with no major improvement in convergence rate compared to a mono-variable preconditioning as represented in Fig. 20. This can also be noticed with the

corresponding condition numbers: 9.55×10^3 for case a, 9.55×10^3 for case b, and 9.56×10^3 for case c.

On the other hand, the last preconditioner taking the cross-dependencies between the void fraction and the phasic velocities into account and accounting for pressure separately leads to much higher convergence rate with less than 10 iterations required. This can also be seen in the condition number being greatly reduced to 3.68. An examination of the eigenvalues estimated assuming cross-dependencies between the void fraction and the phasic velocities and pressure treated separately also demonstrates a perfect match between those eigenvalues and the eigenvalues of the actual full Jacobian. It is also interesting to notice that this result is in accordance with how fluid dynamics calculations are typically carried out in system codes (i.e. not relying on JFNK approaches): the void fraction and phasic velocities are solved together, assuming a given pressure distribution. Pressure is then updated, and the process is repeated until convergence.

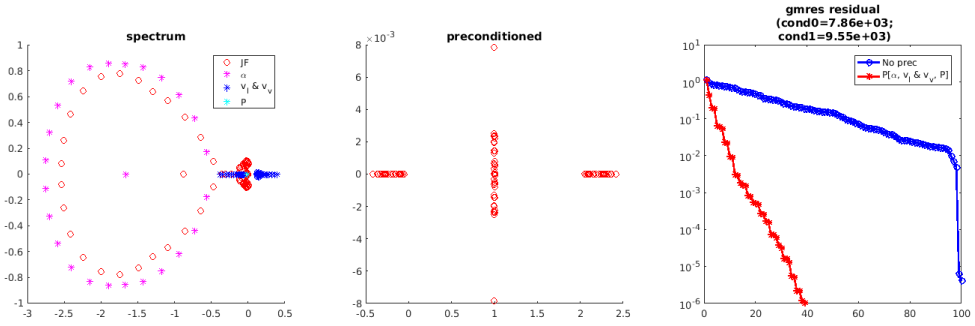

Fig. 21 Effect of preconditioning the void fraction and pressure separately and the phasic velocities together.

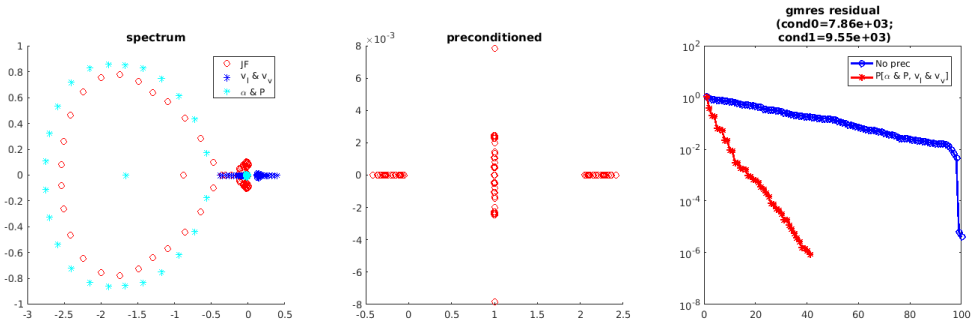

Fig. 22 Effect of preconditioning the void fraction and pressure together and the phasic velocities together.

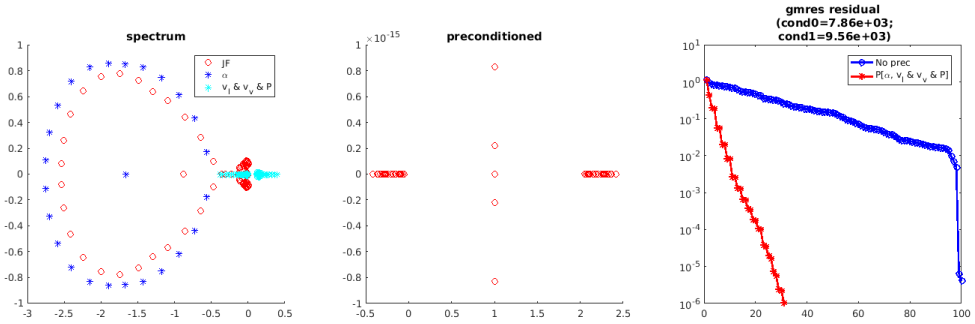

Fig. 23 Effect of preconditioning the void fraction separately and the phasic velocities and pressure together.

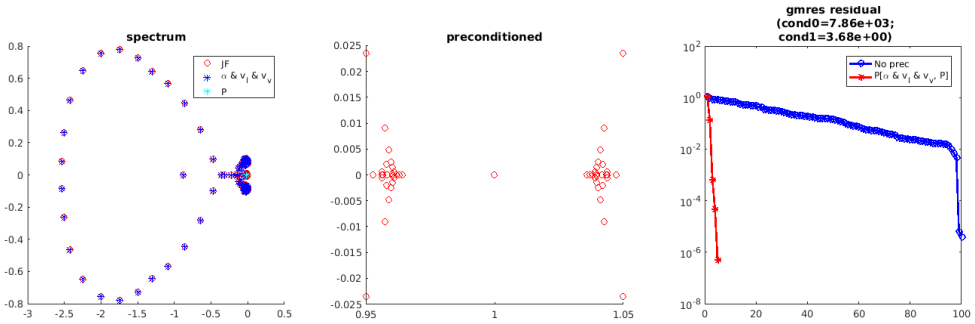

Fig. 24 Effect of preconditioning the void fraction and phasic velocities together and the pressure separately.

One can then conclude that an efficient preconditioner for a monolithic JFNK approach should be designed as follows:

- Preconditioning of the neutron transport solver separately.
- No preconditioning of the heat transfer solver.
- Preconditioning of the fluid dynamics solver separately, with the cross-dependencies between the void fraction and the phasic velocities taken into account.

As a means of verification, the recommendations above were also applied to the analytical Jacobian earlier developed. The corresponding residuals are given in Fig. 25. Compared to Fig. 17 where a numerical Jacobian was used, one notices that the analytical Jacobian converges in as many Newton iterations, thus demonstrating that the thus proposed simplified version of the analytical Jacobian is efficient. Table 1 also compares the number of GMRES iterations per Newton iterations for three types of preconditioners: a numerical preconditioner, an analytical preconditioner where the coupling from the neutron kinetics to the temperature fields is neglected, and the simplified analytical preconditioner following the recommendations above. Although not as efficient as the numerical Jacobian, one notices that the simplified analytical Jacobian leads to drastic reductions in the number of GMRES

iterations compared to the non-simplified analytical Jacobian. Although the recommendations about the structure of a good preconditioner were based on a numerical estimation of the Jacobian, it should again be pointed out here that using a numerical Jacobian is of little use in a JFNK mindset. The purpose of the analysis was to find the necessary structure of the Jacobian. Once this structure is found, this simplified Jacobian should be estimated using for instance an analytical method. On the other hand, it could also be argued that the computational effort for numerically estimating the simplified Jacobian is smaller than the effort for numerically estimating the full Jacobian.

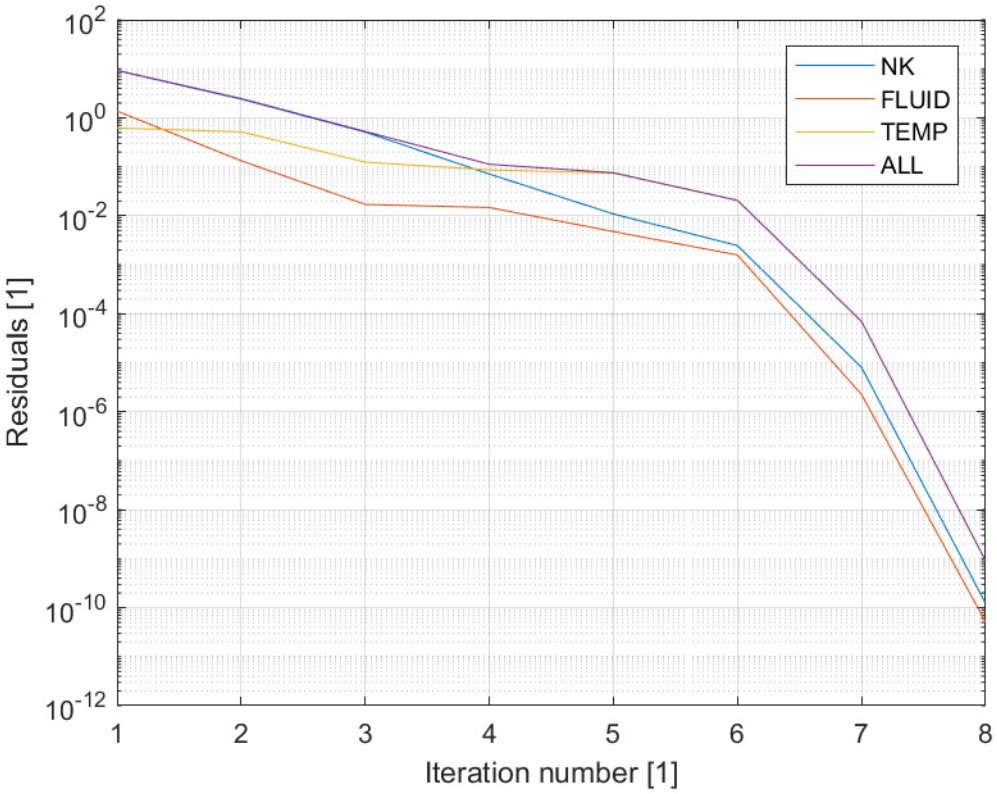

Fig. 25 Actual residuals during multi-physics iterations when the analytical preconditioner is used. The preconditioner is based on separate preconditioning for the neutron transport solver and for the fluid dynamics solver while accounting for the cross-dependencies between void fraction and phasic velocities.

Table 1 Number of GMRES iterations per Newton iterations for various types of preconditioning.

Newton iteration number	Numerical Jacobian	Analytical Jacobian (without coupling from the neutron kinetics to the temperature equations)	Simplified analytical Jacobian
1	1	17	2
2	1	18	5
3	2	50 (max. number allowed)	13
4	3	50 (max. number allowed)	16
5	3	50 (max. number allowed)	20
6	3	50 (max. number allowed)	21
7	3	50 (max. number allowed)	23
8	3	50 (max. number allowed)	30
9		50 (max. number allowed)	
10		50 (max. number allowed)	

d. Approximation of the preconditioner for a "black-box" fluid dynamics solver

Although some recommendations about preconditioning could be made, the development of a simplified analytical preconditioner for the fluid dynamics problem might still represent a difficult task depending on the model and the correlations used. It was thus decided to investigate whether some approximations of the preconditioner could be carried out without relying on the knowledge of the details of the implementation used.

Based on the findings above, it is assumed here that only the cross-dependencies between the void fraction and the phasic velocities need to be resolved, and that the pressure can be treated separately.

When looking at the structure of the fluid dynamics preconditioner and knowing that an upwind first-order spatial discretization scheme was used for the fluid dynamics modelling, the fluid dynamics preconditioner is essentially made of block matrices having two non-zero diagonals (the main diagonal and the "upwind" diagonal next to it). Plotting the dependence of the main diagonal terms and of the off-diagonal terms for each of the retained blocks in the simplified analytical Jacobian for the fluid dynamics as done in Fig. 26, one notices that those term have essentially a linear dependence. Making a linear interpolation using three terms on each diagonal gives a faithful representation of the actual dependence of the main diagonal and off-diagonal terms.

This thus gives the possibility to use such linearly-approximated main diagonal and off-diagonal terms as a preconditioner for the fluid dynamics. The use of such a linearly approximated preconditioner is summarized in Fig. 27. In this figure, the actual Jacobian of

the fluid dynamics problem solely is labelled as “JF”, whereas the Jacobian resulting from the linear approximation described above is referred to as “JF-interp”. As can be seen in this figure, using such a preconditioner combined with a preconditioner for the neutron transport problem leads to a very acceptable efficiency of the preconditioning, with a number of iterations less than 10 and a condition number of 1.34×10^{1}. Although not as efficient as the simplified analytical preconditioner earlier developed (see Fig. 24), the main advantage of this technique lies with the fact that no access to the fluid dynamics model is required and this approach could thus be applied when the fluid solver is used as a “black-box” (i.e. not knowing the details on the fluid dynamics model and implementation). Compared to a full numerical evaluation of the fluid dynamics Jacobian, only three terms per main diagonal and off-diagonal need to be numerically estimated, which represents a significant reduction compared to a full numerical Jacobian.

It has nevertheless to be highlighted that these finding only apply to four-equation model used in this study for the fluid dynamics. Using another more advanced fluid model and correlations might require a different approach. Finally, the structure of the preconditioner is a necessary input to the proposed method.

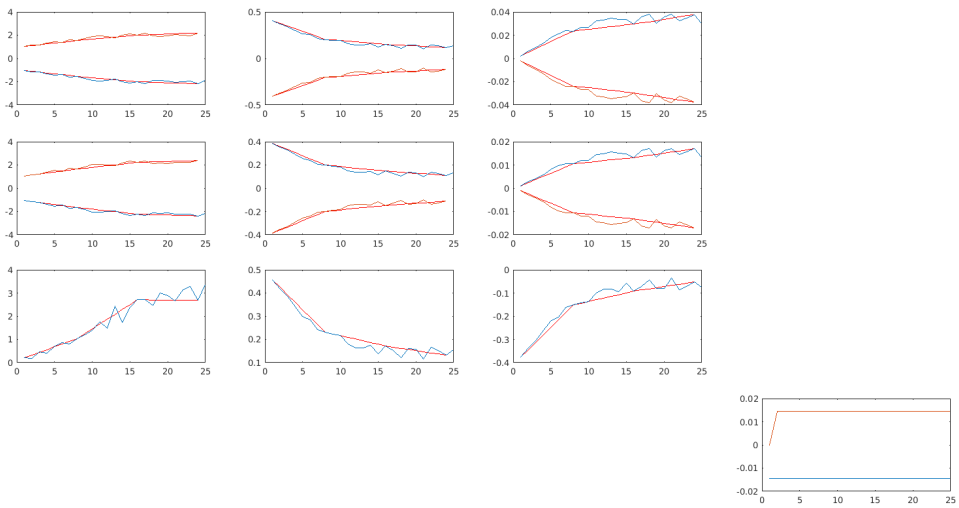

Fig. 26 Dependence of the main diagonal (in blue) and off-diagonal terms (in red) for each of the retained blocks in the simplified preconditioner for the fluid dynamics. A linear interpolation of those terms using three terms on each diagonal is also represented.

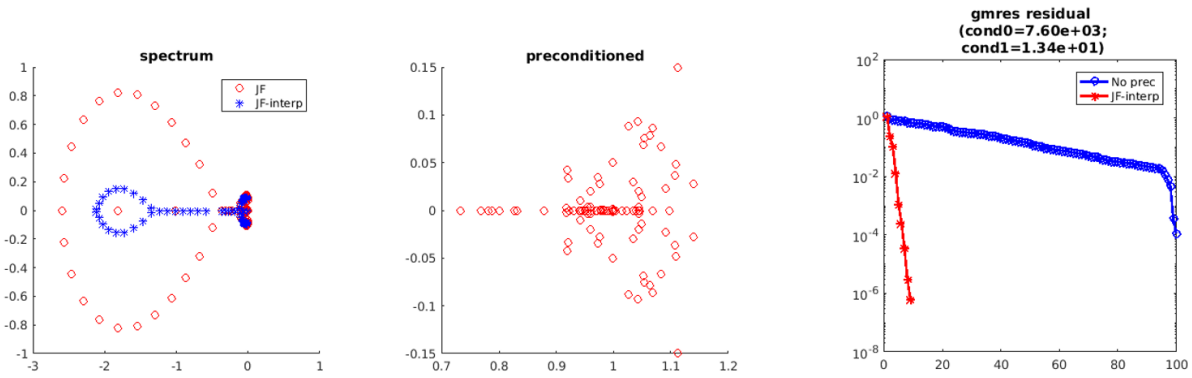

Fig. 27 Effect of preconditioning the void fraction and phasic velocities together and the pressure separately.

6. Generating an initial guess for the Jacobian-Free Newton Krylov monolithic coupling

Although the cases earlier reported in Section 4 converged with an initial guess being arbitrary and far from the converged final solution, various tests of the monolithic JFNK method revealed that the method might have some difficulties in rapidly converging for given sets of initial values.

The purpose of this section is to investigate ways to pre-generate good enough guesses to be subsequently used in a monolithic JFNK approach. Two strategies were considered:

(a) Either using a non-linear Gauss-Seidel approach.
(b) Or using a non-linear Jacobi approach.

In the first case, the equations are solved one after the other, starting with the neutron transport solver, then the fluid dynamics solver, and finally the heat transfer solver. Each time an equation is solved, the corresponding fields in all equations are updated. In the latter case, the equations are also solved one after the other, starting with the neutron transport solver, then the fluid dynamics solver, and finally the heat transfer solver. Nevertheless, the update of the fields is not performed before an entire sweep through all equations is complete. None of the approaches require rewriting the set of balance equations to be later solved by the JFNK method. Only the numerical technique used to solve this set of equations is modified (either non-linear Gauss-Seidel or non-linear Jacobi).

Fig. 28 represents the convergence rate of the non-linear Gauss-Seidel approach and of the non-linear Jacobi approach. In both approaches, a damping factor was also applied for the neutronic solution (as defined in Eq. (37)) and set to $\theta = 0.7$. It can be noticed from this figure that because the update of the fields in the non-linear Jacobi approach is lagging compared with the update of the fields in the non-linear Gauss-Seidel approach, the non-linear Gauss-Seidel approach converges faster than the non-linear Jacobi approach. The non-linear Gauss-Seidel approach should thus be a better initialization technique to a monolithic JNFK method. Fig. 28 also gives the convergence rate of using such an initialization technique (for the first three iterations) before switching to a monolithic JFNK technique. In this test, the JNFK technique converged in five Newton iterations.

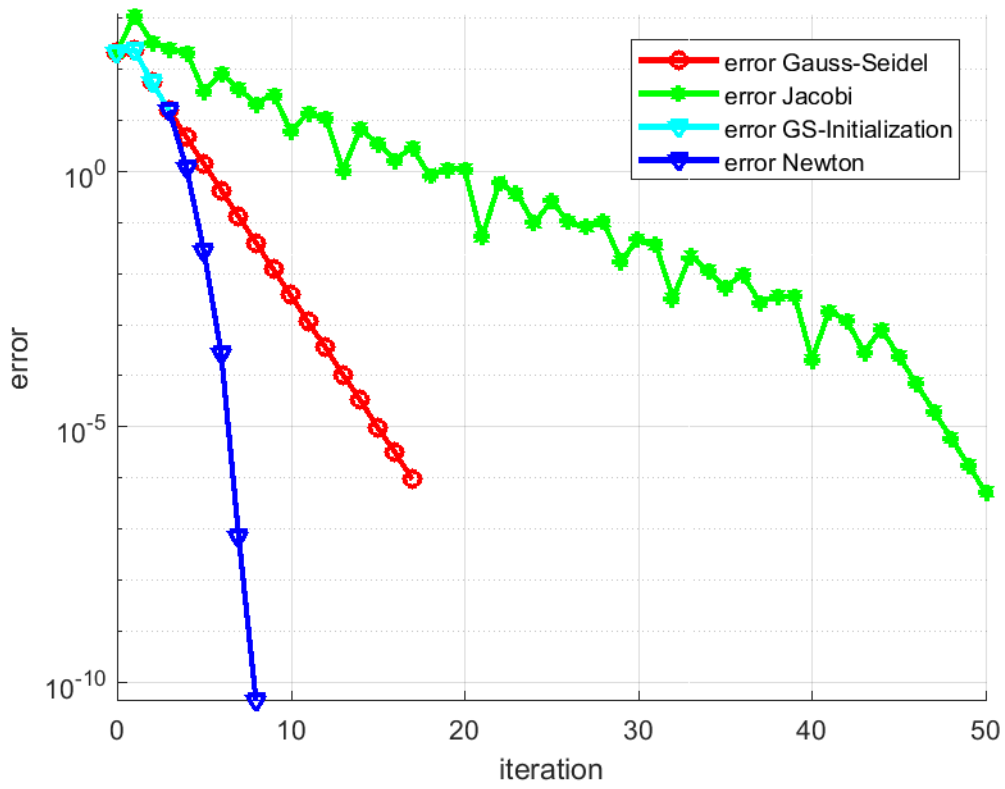

Fig. 28 Comparisons between the non-linear Gauss-Seidel method and the non-linear Jacobi method. The figure also represents using a non-linear Gauss-Seidel initialization technique to a JNFK monolithic coupling.

7. Conclusions and recommendations

In this report, the use of JFNK methods for steady-state coupled calculations representative of BWR systems was considered. In order to keep the system of equations as simple as possible but still retain modelling options specific to BWR conditions, the governing equations were based on the following models:

- Neutron transport modelling relying on two-group diffusion theory, with macroscopic nuclear cross-sections and diffusion coefficients depending on coolant density and fuel temperature.
- Fluid dynamics modelling relying on a four-equation formulation (mixture model with the Zuber and Findlay drift flux model). The correlations in the drift flux model were entirely expressed as functions of the void fraction for the following flow regimes: bubbly flow, churn flow and slug flow. Annular flow regimes were not considered as regards the drift flux model. Pressure drops due to friction were taken into account using the method of Lockhart-Martinelli.
- Heat transfer modelling relying on radially-averaged temperatures on the fuel and cladding regions, respectively. The outer cladding temperature was also explicitly resolved. Correlations from the open literature were used for the fuel pellet thermal conductivity, the gap conductance, the cladding thermal conductivity. Chen's correlation was used for the coolant heat transfer coefficient.

When comparing the operator splitting coupling to the JFNK per physics coupling, it was found that both methods lead to essentially the same behaviour and convergence rate. Due to the inherent strong feedback existing between the coolant density/fuel temperature and the macroscopic data appearing in the neutron transport model, use of a damping technique in the neutron transport solver is absolutely required.

A JFNK monolithic coupling is the only possibility for avoiding the use of any damping. Nevertheless, developing a robust JFNK monolithic coupling requires additional efforts:

- A preconditioner is a necessity. For the coupled model used in this study, it was found that the neutron transport model can be preconditioned separately and that no preconditioning is required for the heat transfer problem. For the fluid dynamics problem, the pressure field can be preconditioned separately, whereas the cross-dependencies between void fraction and phasic velocities need to be resolved in the preconditioner.
- Forcing the initial guess for the JFNK method to be in the neighbourhood of the final solution is highly desirable, in order to guarantee a fast convergence of the JFNK method irrespective of the chosen initial guess. This forcing can be efficiently achieved by using a non-linear Gauss-Seidel technique.

It should be mentioned that a JNFK method can nevertheless represent an efficient method for solving a mono-physics problem as well, providing that an efficient preconditioner is used and that a good enough guess of the solution can be generated.

Based on this study, the following recommendations can also be made:

- If an *à posteriori* coupling of existing codes is to be used, implementing a JFNK per physics coupling has very little advantage. Damping of neutronic oscillation has still to be applied and the convergence rate is essentially similar to an operator splitting coupling. In addition, implementing a JFNK per physics coupling would require massive code rewriting, in order to express the set of equations in a form suitable for being used in a JFNK approach. Considering the extensive V&V efforts spent on the existing nuclear engineering software, the required modifications for a JFNK per physic coupling make little sense considering the almost identical performance of an operator splitting coupling and a JFNK per physics coupling.
- If a completely new software must be developed, a JFNK monolithic coupling is the strategy to be preferred, since it provides a much better control of the residuals for the entire multi-physic problem without any need to use damping, thus leading to faster convergence. Nevertheless, some good enough initial guess need to be provided to the solver, using for instance a non-linear Gauss-Seidel approach. What is far more important is the necessity to precondition the problem. Preconditioning is specific to the set of equations being used. In the present model, it was found that the structure of the preconditioner could be greatly simplified, with a separate preconditioner for neutron transport, no preconditioner for heat transfer, and preconditioner for the fluid dynamics resolving the cross-dependencies between void fraction and phasic velocities together and the pressure field separately. It was also demonstrated that based on this structure of the preconditioner, a simplified preconditioner for the fluid dynamics could be used, either using linearized equations in a simpler formalism (HEM, i.e. with no slip between the phases) or using a "black-box" preconditioner based on linear interpolations on the diagonals of the Jacobian numerically evaluated for a small number of terms on those diagonals.

Although the use of JFNK monolithic coupling seems very appealing, the key component of this techniques lies in efficient preconditioning. It would be highly desirable to test whether the findings of this work are still applicable to much more sophisticated and complex models, such as pure neutron transport versus diffusion theory, and a 6-equation model versus a 4-equation model for the thermal-hydraulics for instance. In particular, one should determine whether a linearized simplified model (such as the HEM for the fluid dynamics) still represent an efficient preconditioner. Moreover, the possibility to use a "black-box" preconditioner would need to be looked at. It should also be pointed out that the findings of this work are based on a chosen spatial discretization. A sensitivity to spatial discretization would be required as well.

Finally, using other coupling approaches, such as Andersson mixing, could represent an interesting alternative, since this method could still use an *à posteriori* coupling of existing codes without any damping to be used [2]. As a result, convergence could be greatly improved.

8. Acknowledgements

This work was supported by the Nordic Thermal-Hydraulic Network – NORTHNET (X-TREAM project – contract numbers 4500297145 with Forsmarks Kraftgrupp AB, 4500056499 with OKG AB, 634282-052 with Ringhals AB, SSM2013-2195 with SSM, and 4500609943 with Westinghouse Electric Sweden AB) and by the Swedish Research Council – Vetenskapsrådet VR (DREAM4SAFER project – contract number C0467701).

9. References

[1] M. Calleja, Investigation of efficient and reliable numerical algorithms for coupled reactor calculations – X-TREAM project: Task 1a – Survey of the different numerical algorithms used in present computer code. Chalmers University of Technology, technical report, CTH-NT-288, Gothenburg, Sweden (2014).

[2] A. Toth, C.T. Kelley, S. Slattery, S. Hamilton, K. Clarno, and R. Pawlowski, Analysis of Anderson acceleration on a simplified neutronics/thermal hydraulics system. Proc. Int. Conf. Mathematics and Computations (M&C), Supercomputing in Nuclear Applications (SNA) and Monte Carlo (MC), Nashville, TN, USA, April 19-23, 2015, American Nuclear Society (2015).

[3] J.C. Ragusa, V.S. Mhadevan, Consistent and accurate schemes for coupled neutronics thermal-hydraulics reactor analysis. *Nuclear Engineering and Design*, **239**, pp. 566-579 (2009).

[4] M. Calleja, Investigation of efficient and reliable numerical algorithms for coupled reactor calculations – X-TREAM project: Task 1b – Survey of the state-of-the-art numerical techniques for solving coupled non-linear multi-physics equations. Chalmers University of Technology, technical report, CTH-NT-289, Gothenburg, Sweden (2014).

[5] A. Ashrafizadeh, C.B. Devaud, and N.U. Aydemir, A Jacobian-free Newton-Krylov method for thermalhydraulics simulations. *International Journal for Numerical Methods in Fluids*, **77**, pp. 590-615 (2015).

[6] L. Zou, H. Zhao, and H. Zhang, Numerical implementation, verification and validation of two-phase flow four-equation drift flux model with Jacobian-free Newton–Krylov method. *Annals of Nuclear Energy*, **87**, pp. 707-710 (2016).

[7] L. Zou, H. Zhao, and H. Zhang, Application of Jacobian-free Newton–Krylov method in implicitly solving two-fluid six-equation two-phase flow problems: Implementation, validation and benchmark. *Nuclear Engineering and Design*, **300**, pp. 268-281 (2016).

[8] T.J. Ypma, Historical development of the Newton-Raphson method. *SIAM Review*, **37** (4), pp. 531-551 (1995).

[9] Y. Saad, Iterative methods for sparse linear systems – Second edition. SIAM (2003).

[10] Y. Saad and M.H. Schultz, GMRES: A Generalized Minimal Residual algorithm for solving nonsymmetric linear systems. *SIAM Journal on Scientific and Statistical Computing*, **7** (3), pp. 856-869 (1986).

[11] CASMO-4E Extended Capability CASMO-4, User's Manual. SSP-09/442 Rev 0, Restricted Distribution – University Release, Studsvik Scandpower, Inc. (2009).

[12] P. Vinai, C. Demazière, and V. Dykin, Modelling of a self-sustained density wave oscillation and its neutronic response in a three-dimensional heterogeneous system. *Annals of Nuclear Energy*, **67**, pp. 41-48 (2014).

[13] C. Demazière, CORE SIM: A multi-purpose neutronic tool for research and education. *Annals of Nuclear Energy*, **38** (12), pp. 2698-2718 (2011).

[14] N. Zuber and J.A. Findlay, Average volumetric concentration in two-phase flow systems. *Journal of Heat Transfer*, **87**, pp. 453-468 (1965).

[15] C. Demazière, Modelling of nuclear reactors. Textbook, 298 pages, Chalmers University of Technology (2017).

[16] M. Mikofski, IAPWS_IF97 functional form with no slip. MATLAB central https://www.mathworks.com/matlabcentral/ (2014).

[17] J.R. Cooper and R.B. Dooley, Revised release on the IAPWS Industrial Formulation 1997 for the thermodynamic properties of water and steam. The International Association for the Properties of Water and Steam, report IAPWS-IF97(2012), 2012.
[18] N.E. Todreas and M.S. Kazimi, Nuclear systems I: Thermal hydraulic fundamentals. Taylor & Francis, Levittown, USA (1993).
[19] C. Demazière, Physics of nuclear reactors. Textbook, 302 pages, Chalmers University of Technology (2016).
[20] L.S. Tong and J. Weisman, Thermal analysis of pressurized water reactors. American Nuclear Society, La Grande Park, USA (1996).
[21] S. Nakamura, Computational methods in engineering and science with applications to fluid dynamics and nuclear systems. John Wiley & Sons, Inc., New York, USA (1977).
[22] MathWorks, https://www.mathworks.com/help/optim/ug/fsolve.html. Accessed on September 25th, 2017.
[23] D.A. Knoll and D.E. Keyes, Jacobian-free Newton-Krylov methods: a survey of approaches and applications. *Journal of Computational Physics*, **193**, pp. 357-397 (2004).